NATIONAL ADVISORY COMMITTEE FOR AERONAUTICS

WARTIME REPORT

ORIGINALLY ISSUED
July 1945 as
Memorandum Report L5G10

TESTS OF FOUR FULL-SCALE PROPELLERS TO DETERMINE THE EFFECT OF TRAILING-EDGE EXTENSIONS ON PROPELLER AERODYNAMIC CHARACTERISTICS

By Julian D. Maynard and Albert J. Evans

Langley Memorial Aeronautical Laboratory
Langley Field, Va.

NACA

WASHINGTON

MR No. L5G10

NATIONAL ADVISORY COMMITTEE FOR AERONAUTICS

MEMORANDUM REPORT

for the

Air Technical Service Command, Army Air Forces

TESTS OF FOUR FULL-SCALE PROPELLERS TO DETERMINE THE EFFECT OF TRAILING-EDGE EXTENSIONS ON PROPELLER AERODYNAMIC CHARACTERISTICS

By Julian D. Maynard and Albert J. Evans

SUMMARY

Tests of four, 10-foot diameter, two-blade propellers have been made in the Langley 16-foot high-speed tunnel to determine the effect of trailing-edge extensions on propeller aerodynamic characteristics. Two of the propellers had 20-percent extensions; one with a cambered-type, and the other with a straight-type of extension. Another propeller had a 40-percent extension of the straight type, and the characteristics of these propellers are compared with the characteristics of a propeller with no trailing-edge extension. This propeller with no trailing-edge extension, which was used as a basis of comparison, had 16-series blade sections and was similar to the NACA design 10-308-03R except the basic design lift coefficient was changed from 0.3 to 0.5. The effect of various angles of extension on propeller characteristics was not investigated, but a calculation of the theoretical pressure distributions indicates that the extension should be designed to prevent much reduction in critical speed of the blade sections for the design condition.

The propellers were tested on a 2000-horsepower dynamometer at blade angles of 20°, 25°, 30°, 35°, 40°, 45°, 50°, and 55° at the three-quarter radius. A constant rotational speed was used for each test, and the tunnel airspeed was varied from 60 to 460 miles per hour. The results are representative of full-scale constant-speed propeller operation at helical tip Mach numbers below the critical.

The use of an extended trailing edge on a propeller blade was found to be a very effective means of increasing the power absorbed by the propeller with little loss in efficiency. Straight-type trailing-edge extensions of 20 and 40 percent (angle of extension = 6.5° at the 0.7 radius) increased the power coefficient for maximum efficiency an amount almost equal to the percent extension at an advance ratio of 1.0. At values of advance ratio greater than 1.0 the increase in power coefficient becomes smaller; and at values less than 1.0, or in the take-off range, the percent increase in power coefficient is greater than the percent extension.

A 20-percent cambered type of extension increased the power coefficient for maximum efficiency considerably more than a 20-percent straight type of extension over the range of advance ratio from 1.0 to 2.5. However, the propeller with the 20-percent cambered type of extension was from 1 to 3 percent less efficient than the propeller with the 20-percent straight type of extension over this range of advance ratio.

Based on equal power absorption and constant rotational speed, the efficiency of the propellers with trailing-edge extensions was about the same or perhaps greater than the efficiency of the propeller without an extension for a cruising or a high-speed condition of operation at a high power coefficient.

INTRODUCTION

The advantages of hollow-steel construction for propeller blades are becoming generally recognized, and the present trend toward that type of construction is definite. Because the cost of tooling for a hollow-steel blade design is very great, a considerable saving of both engineering time and manufacturing cost can be effected if the aerodynamic design of propellers with hollow-steel blades can be made more flexible by the use of extended trailing edges. Design flexibility can be obtained in two respects: first, the extended trailing edges provide a direct means for increasing propeller solidity and therefore ability to utilize engine power; and second, the angular deflection of the extensions can be varied along the blade with the result that the effective pitch distribution may be made an optimum for any desired

operating condition. By the addition of extended trailing edges to an existing blade design, only one set of manufacturing tools is necessary to produce propellers which can be made to meet a great variety of design operating conditions.

A theoretical analysis has been made in reference 1 which shows that the addition of a trailing-edge extension changes the section airfoil characteristics by an amount dependent upon the length and angle of extension. The analysis presents a method of evaluating these changes in airfoil characteristics, and the method of reference 1 is applied in reference 2 to the calculation of propeller characteristics. Also, in reference 2 the effect of varying the angle of extension along the propeller radius to shift more of the load toward the tip was investigated.

The tests presented here were made at the request of the Air Technical Service Command of the Army Air Forces to determine experimentally the effect of trailing-edge extensions on the aerodynamic characteristics of four, full-scale, two-blade propellers. The blades differed in the amount of trailing-edge extension and also in the type of extended strip. Rotational speeds of 1800, 1300, and 1000 rpm were used at airspeeds ranging from 60 to 460 miles per hour, and the resulting range of advance ratio was representative of conventional propeller operation.

APPARATUS

Propeller dynamometer.- A 2000-horsepower propeller dynamometer, still in the development stage, was used to test the propellers in the Langley 16-foot high-speed tunnel. The dynamometer is powered by two 1000-horsepower electric motors arranged in tandem and coupled together for the present tests so that the power of both motors could be expended through a single propeller. A variable-frequency power supply affords an accurate speed control from 300 to 2100 rpm with a permissible overspeed of 2280 rpm. The motors are supported in a housing in such a way that their casings are free to rotate and also free to move axially with their shafts. The axial and rotational movement is restrained by pneumatic pressure capsules which measure thrust and torque. Thrust pressure is indicated as thrust force by means of pneumatic

Emery scales, and torque pressure as torque by means of liquid manometers. The dynamometer is calibrated with the propeller shaft rotating by applying known thrusts and torques and noting the corresponding readings on the thrust scales and torque manometers. Both measurements give straight-line calibrations. A more detailed description of the dynamometer is given in reference 3. Figures 1 and 2 are photographs of the dynamometer mounted in the test section of the tunnel, and figure 3 is a sketch showing principal dimensions of the fairing and spinner. The shape of the spinner and forebody is such as to produce almost uniform axial flow at free-stream velocity in the plane of the propeller. Pressure orifices are located radially between the stationary fairing and the propeller spinner to afford a correction for any change in spinner-fairing juncture pressure due to the propeller operation.

Propeller blades.- The two-blade Curtiss propellers tested were 10 feet in diameter and will be designated in this report by their Curtiss design numbers, 109374, 109376, 109378, and 109376-modified. The blade-form curves for these designs are shown in figure 4, and figure 5 shows the blade section and theoretical pressure distribution at the 0.7 radius for each design. The theoretical pressure distributions were computed for a lift coefficient of 0.5 by the method described in reference 4. The angle of attack (shown in fig. 5) corresponding to this lift coefficient is different for each blade design and gives some indication of changes in airfoil characteristics caused by the trailing-edge extension. The effect of the angle of extension and length of extension on the characteristics of a propeller blade section are discussed in references 1 and 2. Figure 5 shows that no serious pressure peaks are indicated for the four propeller designs tested. Photographs of the blades are shown in figures 6 to 13, inclusive.

Propeller 109374 with no trailing-edge extension was used as a basis of comparison. The blades of this propeller have the same plan form, thickness distribution, and shank design as NACA blade design 10-308-03R except the basic design lift coefficient has been changed from 0.3 to 0.5. The digits of the NACA blade design number have the following significance: the first two digits represent the propeller diameter in feet, the

third digit is ten times the basic design lift coefficient, the remaining digits in the second group are the thickness ratio in percent at the 0.7 radius, and the digits in the third group represent the solidity per blade at the 0.7 radius. The letter R indicates a blade with a conventional round shank. The NACA 16-series blade sections were used and the propeller was designed to have the "Goldstein" minimum induced-energy-loss loading when operating at a blade angle of 45° at the 0.7 radius and an advance ratio of 2.1.

Propeller 109376 is the same as 109374 except a trailing-edge strip on the blades increases the chords to 140 percent of the chords on the 109374 blades. This trailing-edge strip was formed around straight-line extensions to the mean camber lines which were set up in the following manner: on the layouts for the 109374 blade sections straight lines were passed through the mean camber lines at 50 percent of the basic chords and the center of the trailing-edge radii, and these lines were extended to intersect lines erected perpendicular to the chord lines at 140 percent of the basic chords. Trailing-edge radii of 0.01 inch were then drawn with their centers on these intersections. Through the centers of these radii and tangent to the basic mean camber lines, straight lines were drawn which are the extensions to the mean camber lines referred to above. From the trailing edge of the basic blade section to the trailing edge of the strip the profiles are straight and were faired into the basic profiles at the 90-percent-chord station. This was the original design which was later changed. Calculation of the theoretical pressure distribution for the original design (fig. 5) showed that to attain a lift coefficient of 0.5 it would be necessary for a section at the 0.7 radius to operate at an angle of attack of 2.26°. This increase in angle of attack caused a pressure peak at the nose of the section with a consequent decrease in critical speed. For this reason the trailing-edge strip was changed by increasing the angle between the mean camber line extension and the basic chord line (which varied from 3°27' to 4°0' as originally set up) by 3° for all sections along the radius, and by increasing the trailing-edge radius on the strip to 0.02 inch. For this final design the angle of attack at the 0.7 radius corresponding to a lift coefficient of 0.5 was 1.28°, and the theoretical pressure distribution showed a fairly uniform lift load over most of the section. The angle of extension, which is defined as the acute angle between the

extension and a straight line joining the extremities of the mean camber line of the original airfoil section (chord line for this section), was 6.5° at the 0.7 radius for the final design. Only the final design (109376) was manufactured and tested for this investigation.

Propeller 109378 had chord lengths 120 percent of the chords on the 109374 blades, the additional 20 percent forming a cambered type of extension. The mean camber lines for these wider sections were calculated and laid out for a lift coefficient of 0.5. Then the thickness distribution which would be obtained on a blade with a 20-percent trailing-edge extension set up like the original 109376 design was laid around this mean camber line. The angle of attack of a section at the 7.0 radius corresponding to a lift coefficient of 0.5 was found to be only 0.27° for this design. (See fig. 5.) This indicates that the section airfoil characteristics for the 109378 blade are quite different from those of the basic 109374 blade whose section at the 0.7 radius must operate at 1.35° to attain the design lift coefficient of 0.5. It is realized that the 109378 design does not represent a true trailing-edge extension in the usual sense, although a blade of this type could be manufactured and then its trailing edge cut off to give the required solidity. The results of the tests on this blade are presented mainly because of academic interest.

Propeller 109376-modified was made by simply cutting off the 40-percent trailing-edge extension on the 109376 blades to form a 20-percent extension. This gave the 109376-modified blades the same amount of trailing-edge extension as the 109378 blades, and a comparison of the two designs with equal chord lengths could be made. The angle of extension of the 109376-modified blade was the same as for the 109376 blade, and the angle of attack of a section at the 0.7 radius corresponding to a lift coefficient of 0.5 was approximately the same as for the 109376 blade. This is in agreement with the analysis in reference 1, where it was found that the angle of extension necessary to maintain the same design lift coefficient as the basic airfoil was approximately the same for both the 20- and the 40-percent extensions.

The following table summarizes the distinguishing features of the blade designs just described:

Blade design no.	Type of extension	Length of extension, percent chord	Angle of extension at 0.7 radius (deg)	α at 0.7 radius corresponding to a C_L of 0.5 (calculated, see fig. 5) (deg)
109374	None	----------	----------	1.35
[a]109376 (original)	Straight	40	3.5	2.26
109376 (final)	Straight	40	6.5	1.28
109378	Cambered	20	----------	.27
109376-modified	Straight	20	6.5	1.22

[a]This propeller was not tested.

NATIONAL ADVISORY
COMMITTEE FOR AERONAUTICS

TESTS

Thrust, torque, and rotational speed were measured for each of the four propellers during tests at blade angles of 20°, 25°, 30°, 35°, 40°, 45°, 50°, and 55° at the three-quarter (45-inch) radius. A constant rotational speed was used for each test, and a range of advance ratio $\left(J = \frac{V}{nD}\right)$ was covered by changing the tunnel airspeed, which was varied from about 60 to 460 miles per hour. A rotational speed of 1800 rpm was used for tests at blade angles of 20°, 25°, 30°, and 35°; 1300 rpm for blade angles of 40°, 45°, and 50° (one test was made of propeller 109374 at a blade angle of 40° and 1800 rpm); and 1000 rpm for a blade angle of 55°. At the higher blade angles the dynamometer would not deliver sufficient torque to cover the complete range of advance ratio at the higher rotational speeds, and for this reason the lower rotational speeds were used for the higher blade angles. The single test at a blade angle of 40° and 1800 rpm for propeller 109374 was possible because this propeller had no trailing-edge extension and absorbed less power than the other propellers. Additional tests were made at a constant rotational speed of 1000 rpm for all blade angles in an attempt to obtain propeller characteristics in the range of advance ratio well below that for peak efficiency. At this rotational speed the dynamometer could deliver sufficient torque to obtain data at fairly low values of advance ratio. At the higher rotational speeds the resultant tip speeds obtained simulate actual flight conditions, and the variation of air-stream Mach number with advance ratio is representative of full-scale constant-speed propeller operation.

REDUCTION OF DATA

The test results corrected for tunnel-wall interference and spinner force are presented in the form of the usual thrust and power coefficients and propeller efficiency. The symbols and definitions used throughout this report are as follows:

p pressure difference between a point on the airfoil surface and static pressure in the undisturbed stream, pounds per square foot

q	dynamic pressure $\left(\frac{1}{2}\rho V^2\right)$, pounds per square foot
p/q	pressure coefficient
M	air-stream Mach number
M_t	helical tip Mach number
V	airspeed, feet per second
n	propeller rotational speed, rps
D	propeller diameter, feet
J	propeller advance ratio (V/nD)
ρ	mass density of air, slugs per cubic foot
T	propeller thrust, pounds
C_T	thrust coefficient $(T/\rho n^2 D^4)$
P	power absorbed by the propeller, foot-pounds per second
C_P	power coefficient $(P/\rho n^3 D^5)$
η	propeller efficiency $\left(J\frac{C_T}{C_P}\right)$
C_L	lift coefficient
α	angle of attack, degrees
C_s	speed-power coefficient $\left(\sqrt[5]{\frac{\rho V^5}{Pn^2}}\right)$ or $\left(\frac{J}{\sqrt[5]{C_P}}\right)$
x	fraction of propeller tip radius
β	blade angle, degrees
h	blade section maximum thickness
b	blade width, chord

Definition of propeller thrust.- Propeller thrust, as used in this report, is defined as the shaft tension caused by the spinner to tip portion of the blades rotating in the air stream. The indicated propeller thrust has been corrected by the amount of the tare thrust found in operating the dynamometer and spinner without propeller blades at the same values of rotational speed and airspeed as were used in the propeller tests. A further correction was made for the fictitious thrust due to the influence of the pressure field of the propeller acting at the juncture between the spinner and the stationary fairing. The change in spinner thrust due to a change in pressure at the spinner-fairing juncture varied with propeller operating conditions and was determined from pressure measurements in the juncture between the propeller spinner and the fairing at the rear of the propeller. Values of thrust coefficient were changed by no more than 0.005 by this correction to the spinner thrust.

Correction for wind-tunnel-wall interference.- The flow past the propeller is constrained by the walls of the tunnel, and the axial velocity which occurs in front of the propeller in the wind tunnel differs from that which would occur in free air when the propeller is producing the same thrust and torque at the same rate of rotation as used in the wind tunnel. A correction must be applied to the tunnel datum velocity to obtain the corresponding free-stream airspeed. Glauert, in reference 5, has made an analysis in which he shows this correction to be a function of the ratio of propeller thrust to dynamic pressure, or ratio of thrust coefficient to nominal advance ratio. This correction, which was used for the data obtained in these tests, amounted to less than 3 percent for most of the data and to less than 1 percent for data in the region of peak efficiency.

RESULTS AND DISCUSSION

Faired curves of thrust coefficient, power coefficient, and propeller efficiency plotted against advance ratio are presented in figures 14 through 25 for the four propellers tested. Test points are shown on the figures giving thrust and power coefficients. Several tests were repeated during the test program and the results were found to agree within 1 percent. Comparative data in

figures 14 through 25, therefore, are presented as accurate to within 1 percent.

The results of the tests made at a constant rotational speed of 1000 rpm were not consistent, especially in the range of advance ratio for peak efficiency. This inaccuracy was due to a mechanical difficulty with the dynamometer and will be eliminated in future propeller tests. Only a portion of the data obtained at this lower rotational speed is presented in figures 26, 27, 28, and 29 to show the region of stalled flutter for the four propellers tested. The flutter was detected by sound and occurred when the blades were operating in a stalled condition.

Figure 30 is included to show the variation of airstream Mach number and helical tip Mach number with advance ratio for the different rotational speeds used in the tests.

The effect of rotational speed on propeller characteristics.- A difference in the slope of both the thrust- and power-coefficient curves at the different test rotational speeds is shown in figures 14 to 25. This difference in slope may be attributed to a change in the airfoil characteristics of the blade sections with change in Reynolds number or, more likely, Mach number; however, the values of peak efficiency were little affected at Mach numbers below the critical. Characteristic curves of propeller 109374 at 1800 and 1300 rpm and a blade angle of 40° are compared in figures 14, 15, and 16. In the range of advance ratio of the test at the higher rotational speed the helical tip Mach number varied from 0.94 to 1.0, and the loss in efficiency shown in figure 16 may be attributed to compressibility effects. The decrease in the value of advance ratio for zero thrust and power coefficients shown in the test at the higher rotational speed is not readily explained. Drag variation alone cannot account for the effect, because drag curve variation would tend to have the opposite effects on thrust- and power-coefficient values. A variation of the angle for zero lift of the blade sections, or perhaps some Reynolds number effect, is indicated.

To illustrate the effect of Mach number on the airfoil characteristics of the 109374 propeller, Lock's

simplified inverse method for calculating airfoil characteristics from propeller data (reference 6) was used to determine the variation of lift coefficient with angle of attack for two rotational speeds used in the tests. Figure 31 shows that the slope of the lift curve increases with an increase in rotational speed, and the trend of the data shown compares favorably with airfoil data for 16-series sections reported in reference 7. The lift coefficient curves shown in figure 31 are not presented for use as airfoil data, but for purposes of illustration only. The variation of helical tip Mach number with angle of attack is also shown in figure 31 for the two rotational speeds.

The effect of trailing-edge extensions on maximum efficiency and power coefficient for maximum efficiency.- A comparison of the envelope curves of propeller efficiency shown in figure 32 indicates that the trailing-edge extensions caused only small changes in propeller efficiency. The 40-percent straight-type trailing-edge extension on propeller 109376 caused very little change in efficiency over most of the range of advance ratio except the lower values where the loss was about $2\frac{1}{2}$ percent. Propeller 109376 with the original trailing-edge extension cut to form a 20-percent extension (109376-modified) is about 1 percent more efficient over part of the range of advance ratio than propeller 109374 with no trailing-edge extension. This indicated increase in efficiency, however, is within the experimental error. Propeller 109378 with the 20-percent cambered-type trailing-edge extension is $1\frac{1}{2}$ to $2\frac{1}{2}$ percent less efficient over most of the range of advance ratio than propeller 109374 with no trailing-edge extension. This loss in efficiency becomes less as the advance ratio increases.

Also in figure 32 are curves showing the power coefficient for maximum efficiency for the four propellers tested. These curves indicate that for a relatively large increase in power coefficient due to the trailing-edge extension there is only a small decrease in propeller efficiency, and perhaps an increase in efficiency at the higher values of advance ratio for the 109376-modified propeller. In figure 33 the increase in power coefficient for maximum efficiency caused by the 20-percent straight-type trailing-edge extension (109376-modified) is compared with the increase caused

by the 20-percent cambered-type of extension (109378). The cambered type of extension increased the power coefficient for maximum efficiency considerably more than the straight type of extension over the range of advance ratio from 1.0 to 2.5. However, the propeller with the 20-percent cambered type of extension was from 1 to 3 percent less efficient than the propeller with the 20-percent straight type of extension over this range of advance ratio. The difference in power absorption qualities of the two propellers with 20-percent trailing-edge extensions may be attributed to the difference in airfoil characteristics of the blade sections.

Figure 34 shows the effect of the amount of trailing-edge extension on the increase in power coefficient for maximum efficiency caused by the straight type of extension on propellers 109376 and 109376-modified. The percent increase in power coefficient is almost equal to the percent extension at an advance ratio of 1.0. At values of advance ratio greater than 1.0 the increase in power coefficient becomes smaller; and at values less than 1.0, or in the take-off range, the percent increase in power coefficient is greater than the percent extension.

Constant power propeller operation.- Figure 35 shows a comparison of the power coefficients for the four propellers tested. Because the propellers have widely different power absorption qualities, as shown in figure 35, and because an airplane propeller often operates over an extensive range of advance ratio at constant rotational speed and torque, the data were analyzed at several different values of constant power coefficient and constant rotational speed. The results of this analysis, presented in figure 36, provide a better comparison of the effect of the trailing-edge extensions on efficiency. In the range of advance ratio of the tests the trailing-edge extensions caused only small changes in efficiency except at high advance ratios and a very low value of constant power coefficient. For a cruising or high-speed condition of operation at a high power coefficient (constant power coefficient of 0.2, constant rotational speed of 1300 rpm, and range of advance ratio from 1.7 to 2.8) the efficiency of the propellers with trailing-edge extensions was about the same or perhaps greater than the efficiency of the propeller without an extension. Although the range of advance ratio of the tests is limited, the trend of the data in figure 36 indicates that as the power coefficient increases the loss in

efficiency caused by the trailing-edge extensions becomes less; and at low values of advance ratio there will perhaps be a gain in efficiency for high power coefficients. A propeller whose solidity has been increased by extending the trailing edge will perhaps be more efficient for the take-off and climb conditions of operation, particularly for high power coefficients. This effect of solidity is borne out by the tests reported in reference 8. Based on equal power absorption and constant rotational speed, propeller 109376-modified with the 20-percent straight-type extension was more efficient for a high-speed condition of operation than propeller 109378 with the 20-percent cambered-type extension, or propeller 109376 with the 40-percent straight-type extension.

Speed-power coefficient charts.- Comparison of the propellers on the basis of C_s may be more practical from the viewpoint of a designer because this coefficient represents the actual design conditions of power, rotational speed, and airspeed. For this reason the design charts in figures 37, 38, 39, and 40 are included. Also, the composite skeleton C_s chart in figure 41 is presented to serve as an aid in the selection of a propeller for a particular design condition. In figure 41 the envelopes of the efficiency curves were taken from figures 37 to 40, inclusive, and comparison shows that the order of merit for the four propellers is the same when based on speed-power coefficient as when based on advance ratio. The curves in figure 41 give the propeller efficiency for any given set of design conditions, that is, airspeed, engine power, propeller rotational speed, and air density.

CONCLUSIONS

High-speed tunnel tests of four, full-scale, two-blade propellers to determine the effect of trailing-edge extensions on propeller aerodynamic characteristics in a range of helical tip Mach numbers below the critical lead to the following conclusions:

1. Extension of the trailing edge of a propeller blade greatly increases the power absorption qualities of the propeller with little loss in efficiency.

2. A 20-percent cambered type of extension increased the power coefficient for maximum efficiency considerably more than a 20-percent straight type of extension over the range of advance ratio from 1.0 to 2.5. However, the propeller with the 20-percent cambered type of extension was from 1 to 3 percent less efficient than the propeller with the 20-percent straight type of extension over this range of advance ratio.

3. Straight-type trailing-edge extensions of 20 and 40 percent (angle of extension = 6.5° at the 0.7 radius) increased the power coefficient for maximum efficiency an amount almost equal to the percent extension at an advance ratio of 1.0. At values of advance ratio greater than 1.0 the increase in power coefficient becomes smaller; and at values less than 1.0, or in the take-off range, the percent increase in power coefficient is greater than the percent extension.

4. Based on equal power absorption and constant rotational speed, the efficiency of the propellers with trailing-edge extensions was about the same or perhaps greater than the efficiency of the propeller without an extension for a cruising or a high-speed condition of operation at a high power coefficient.

5. Based on equal power absorption and constant rotational speed, propeller 109376-modified with the 20-percent straight-type extension was more efficient for a cruising or a high-speed condition of operation than propeller 109378 with the 20-percent cambered-type extension, or propeller 109376 with the 40-percent straight-type extension.

Langley Memorial Aeronautical Laboratory
National Advisory Committee for Aeronautics
Langley Field, Va.

REFERENCES

1. Theodorsen, Theodore, and Stickle, George W.: Effect of a Trailing-Edge Extension on the Characteristics of a Propeller Section. NACA ACR No. L4I21, 1944.

2. Crigler, John L.: The Effect of Trailing-Edge Extension Flaps on Propeller Characteristics. NACA ACR No. L5A11, 1945.

3. Corson, Blake W., Jr., and Maynard, Julian D.: The Effect of Simulated Icing on Propeller Performance. NACA TN No. 1084, 1946.

4. Theodorsen, T., and Garrick, I. E.: General Potential Theory of Arbitrary Wing Sections. NACA Rep. No. 452, 1933.

5. Glauert, H.: The Elements of Aerofoil and Airscrew Theory. American ed., The MacMillan Co., 1943, pp. 222-226.

6. Lock, C. N. H.: A Graphical Method of Calculating the Performance of an Airscrew. R. & M. No. 1849, British A.R.C., 1938.

7. Stack, John: Tests of Airfoils Designed to Delay the Compressibility Burble. NACA TN No. 976, Dec. 1944. (Reprint of ACR, June 1939.)

8. Biermann, David, Gray, W. H., and Maynard, Julian D: Wind-Tunnel Tests of Single- and Dual-Rotating Tractor Propellers of Large Blade Width. NACA ARR, Sept. 1942.

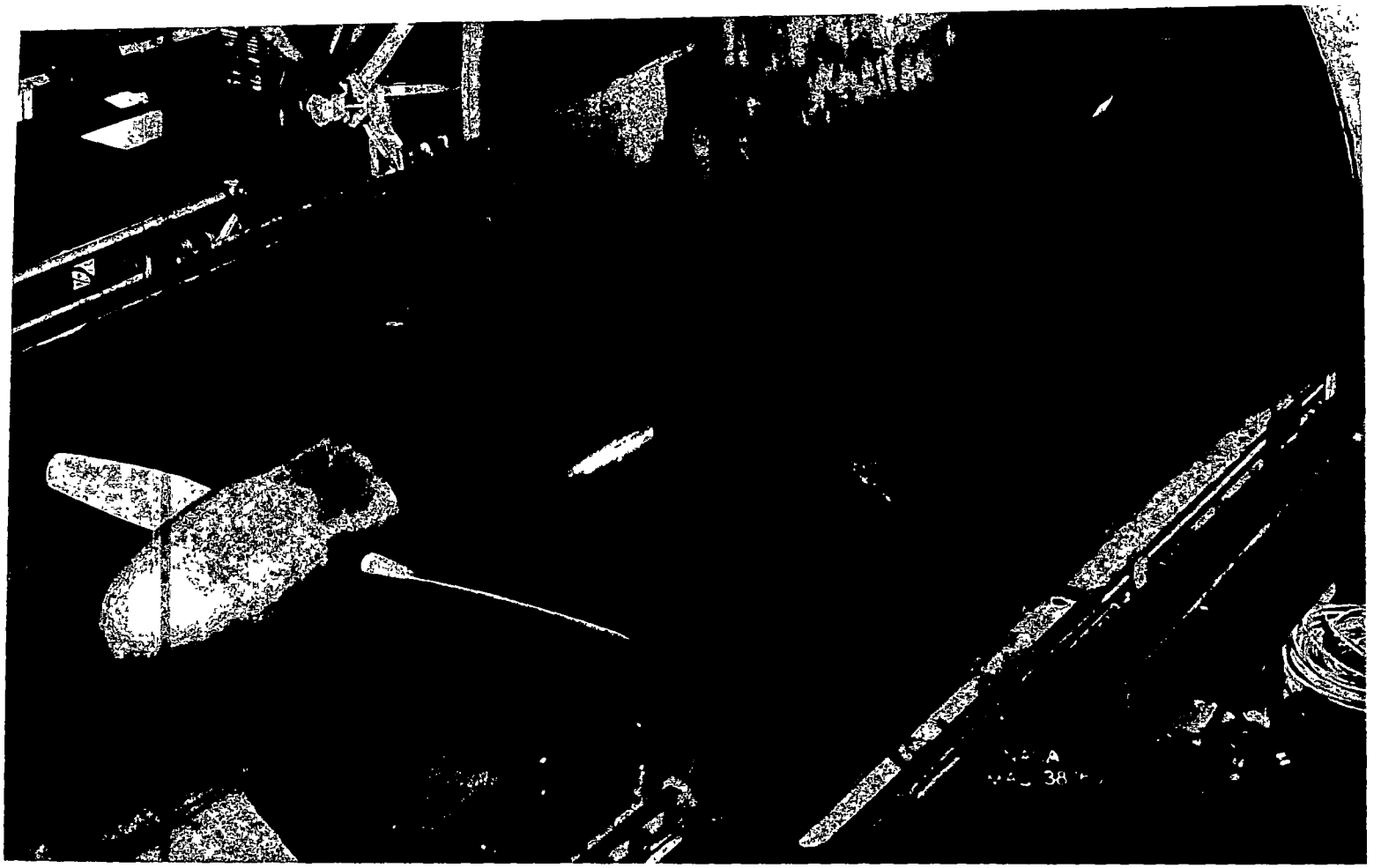

Figure 1.- Propeller dynamometer in test section, blades with no trailing-edge extension, tunnel open.

MR No. L5G10

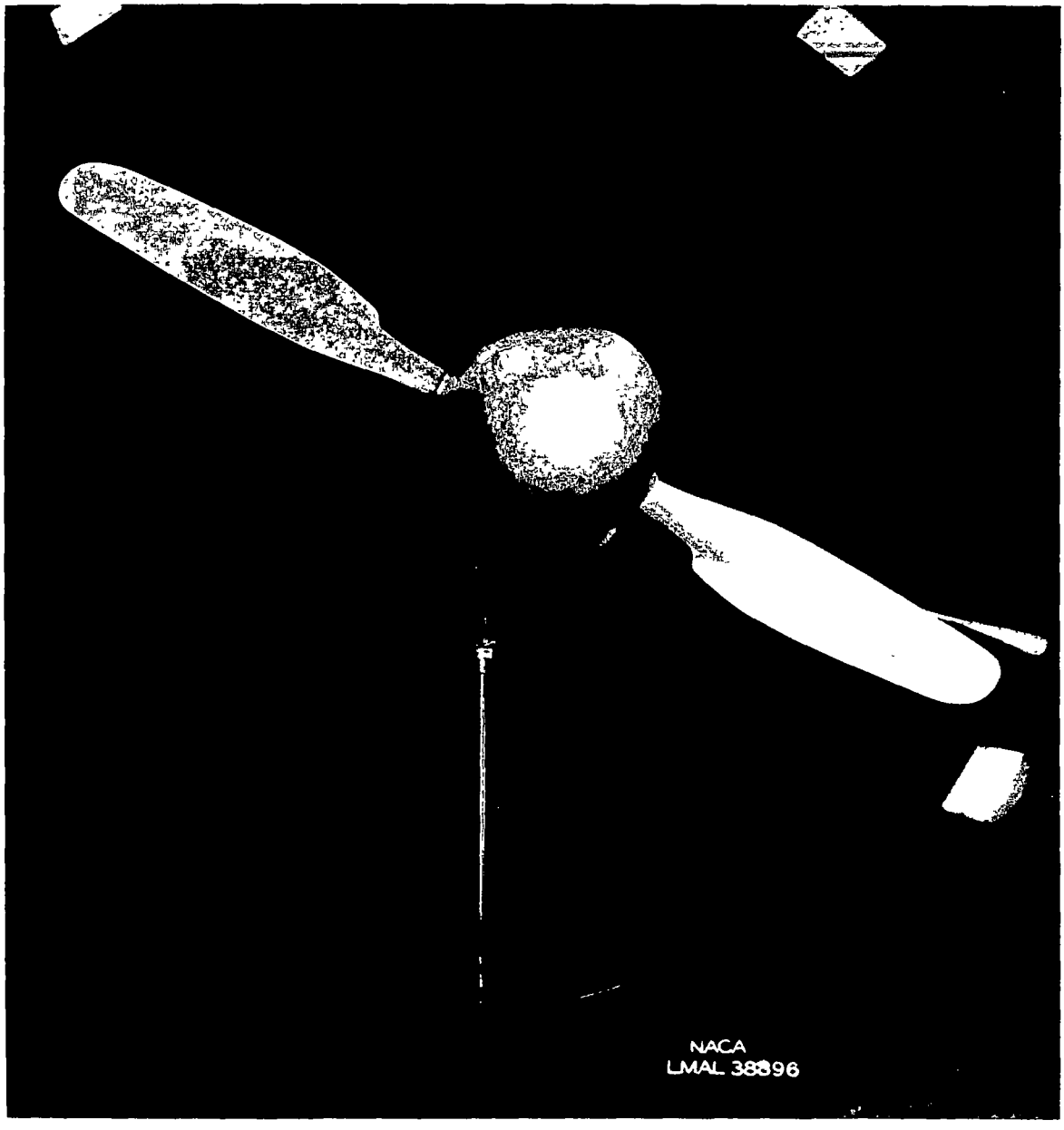

Figure 2.- Propeller dynamometer in test section, 40-percent trailing-edge extension blades.

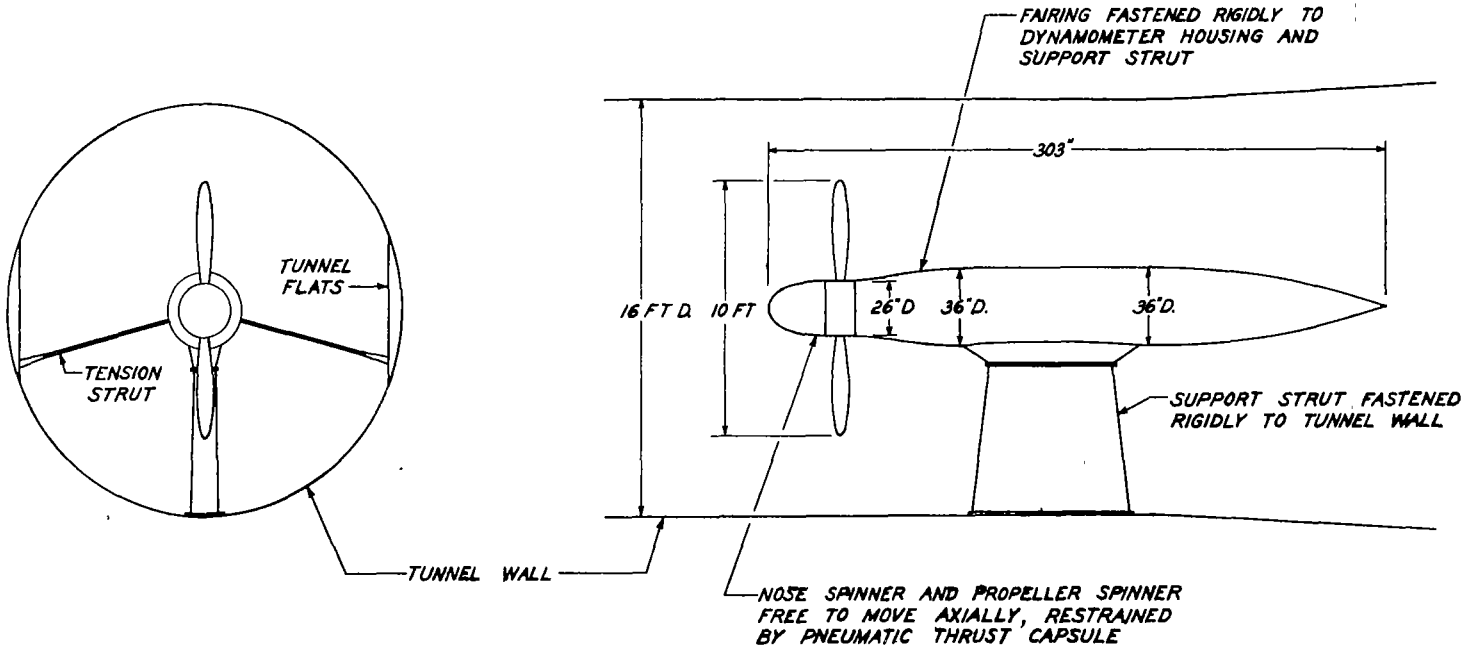

FIGURE 3.—CONFIGURATION OF DYNAMOMETER FOR TESTS OF PROPELLER BLADES WITH TRAILING EDGE EXTENSIONS.

MR No. L5G10

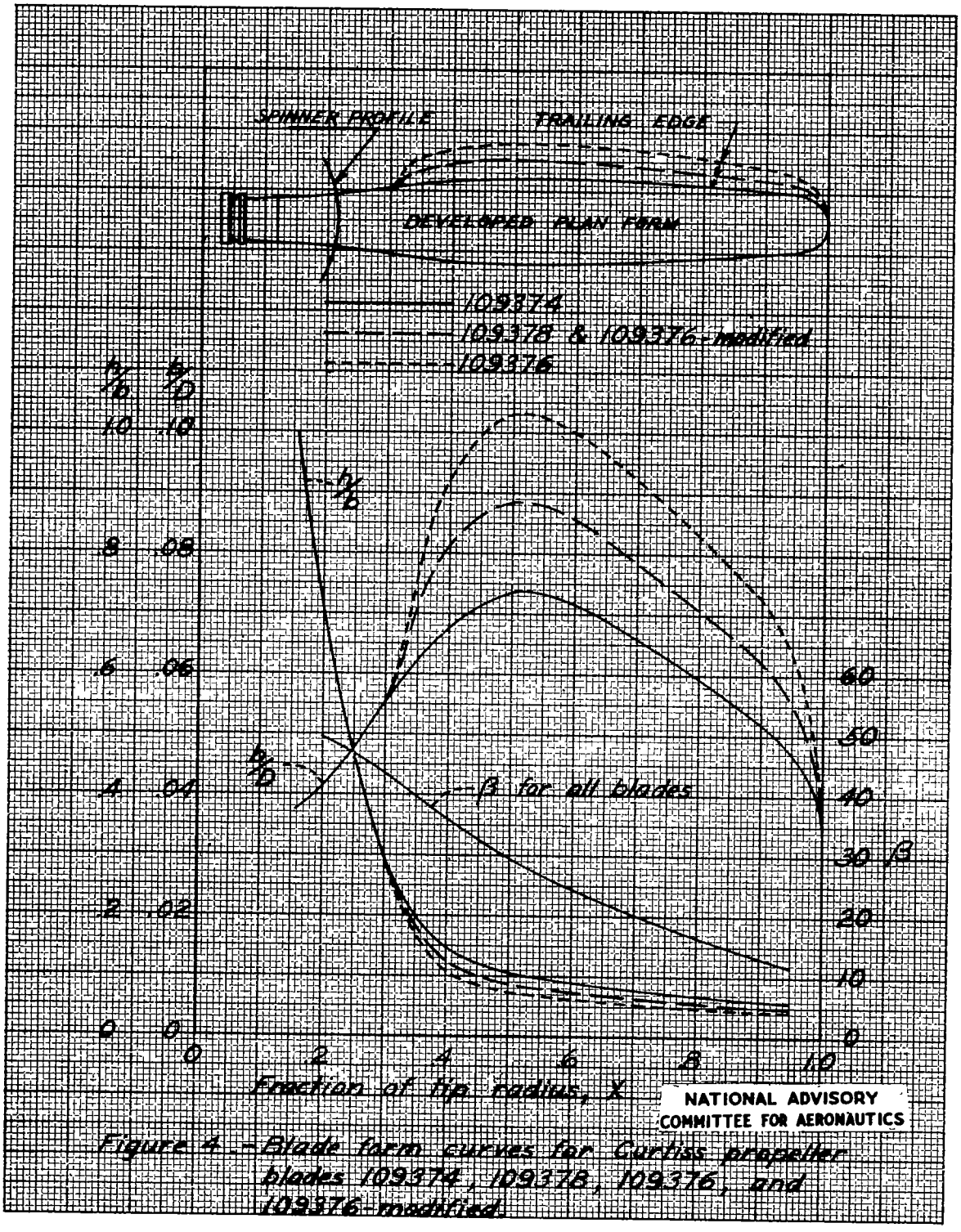

Figure 4.--Blade form curves for Curtiss propeller blades 109374, 109378, 109376, and 109376-modified.

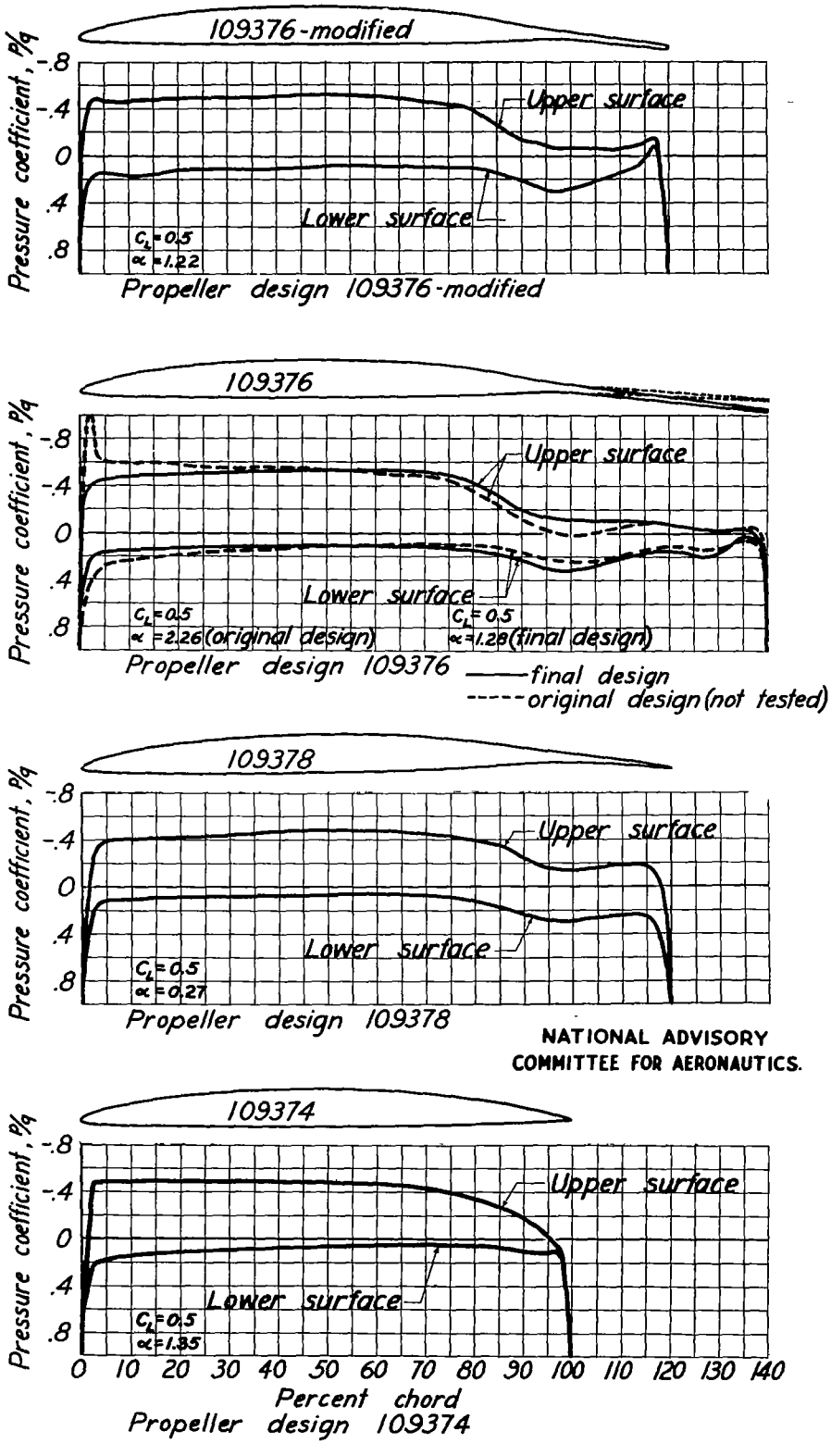

Figure 5.— Blade section and theoretical pressure distribution at the 0.7 radius for each propeller design.

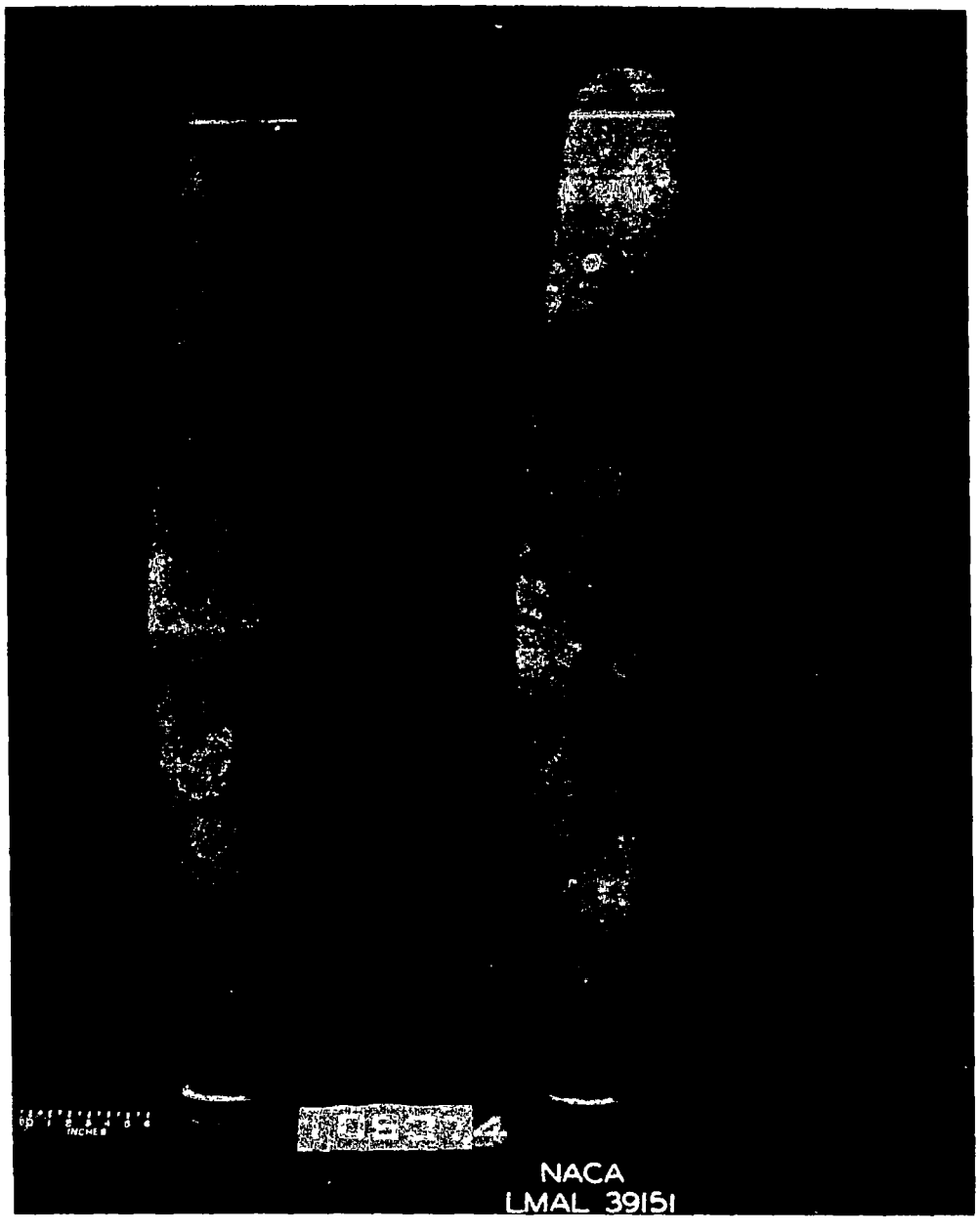

Figure 6.- Propeller blades 109374 (no trailing-edge extension) - thrust face (lower surface).

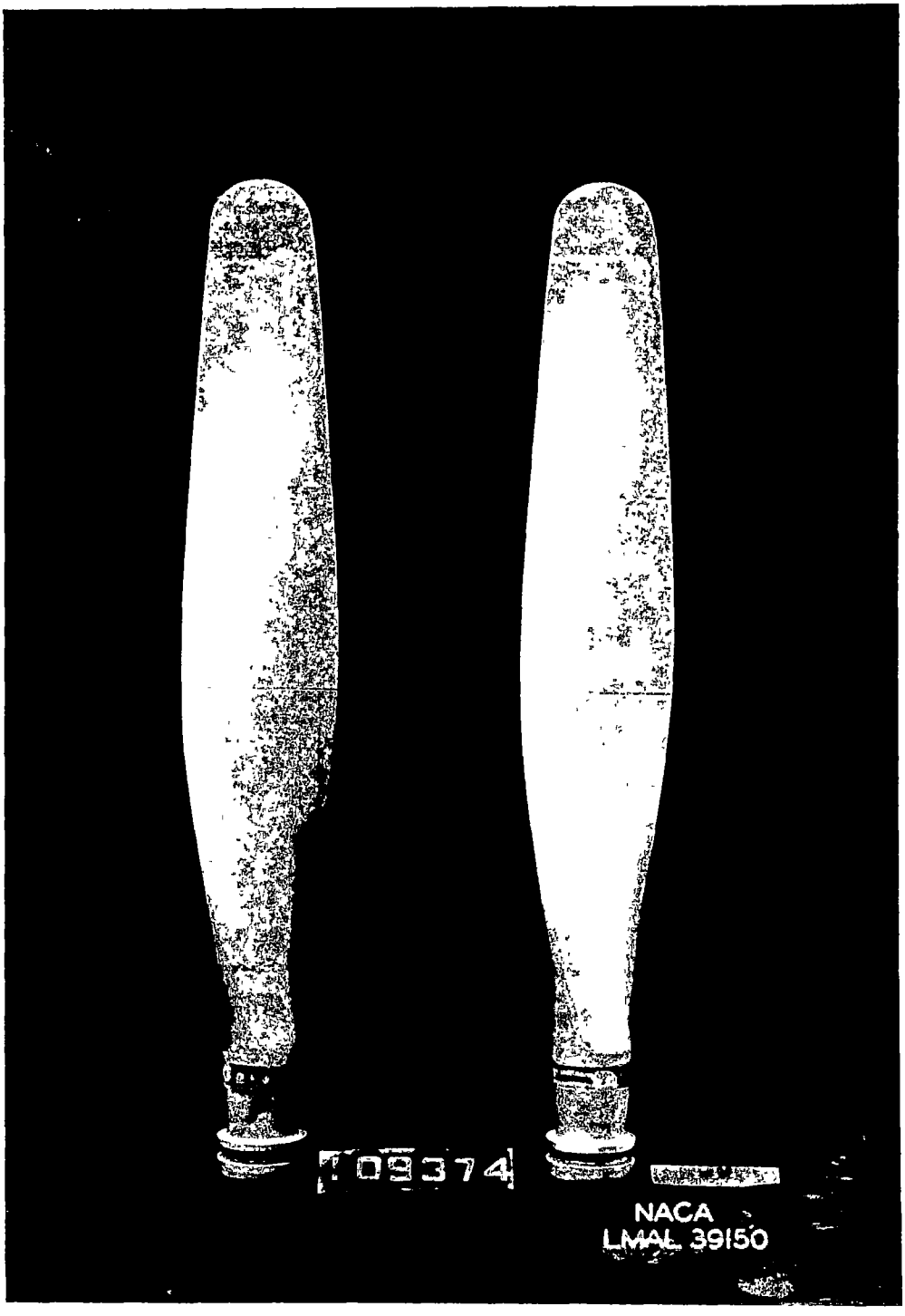

Figure 7.- Propeller blades 109374 (no trailing-edge extension) - cambered face (upper surface).

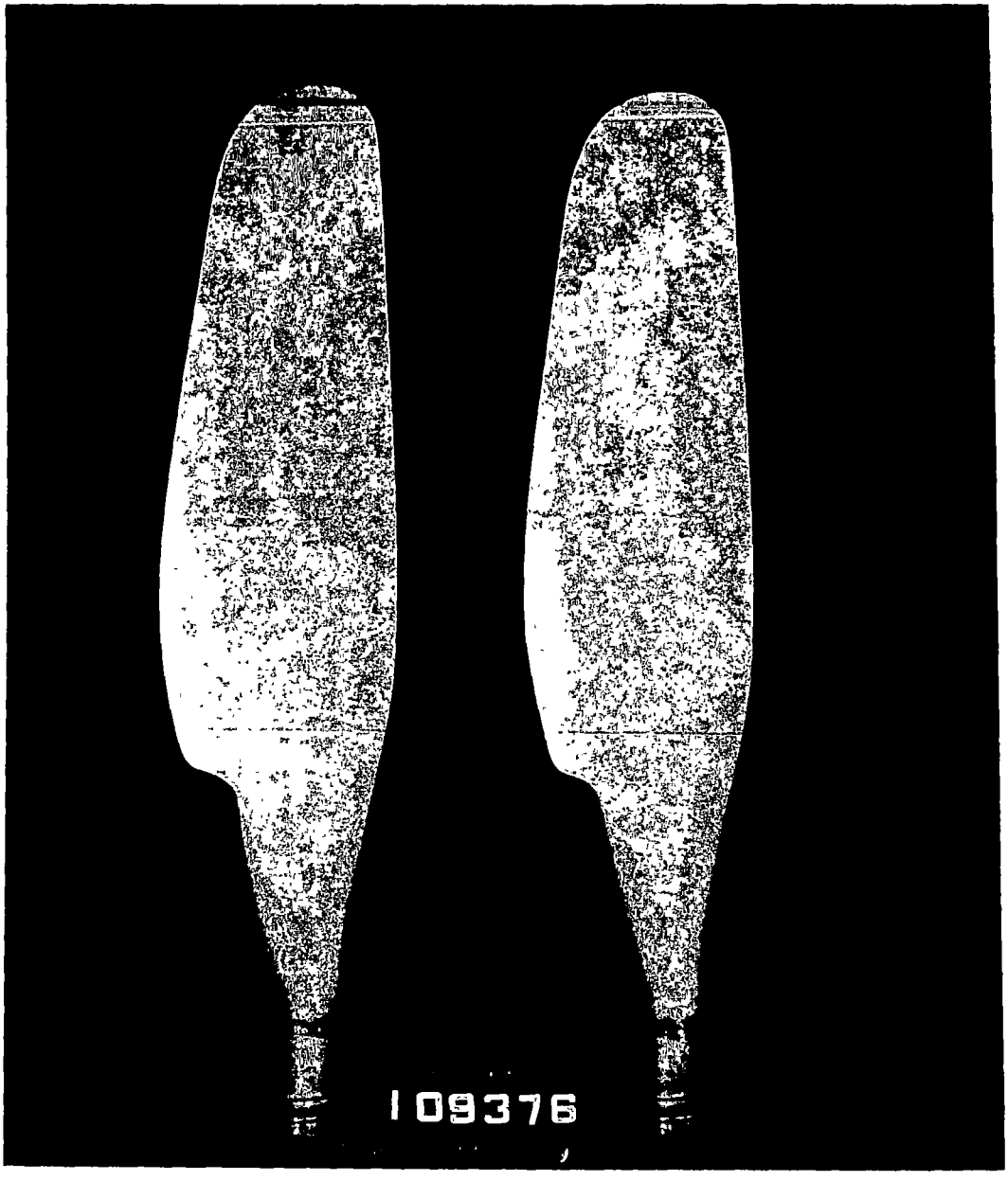

Figure 8.- Propeller blades 109376 (40-percent trailing-edge extension) - thrust face (lower surface).

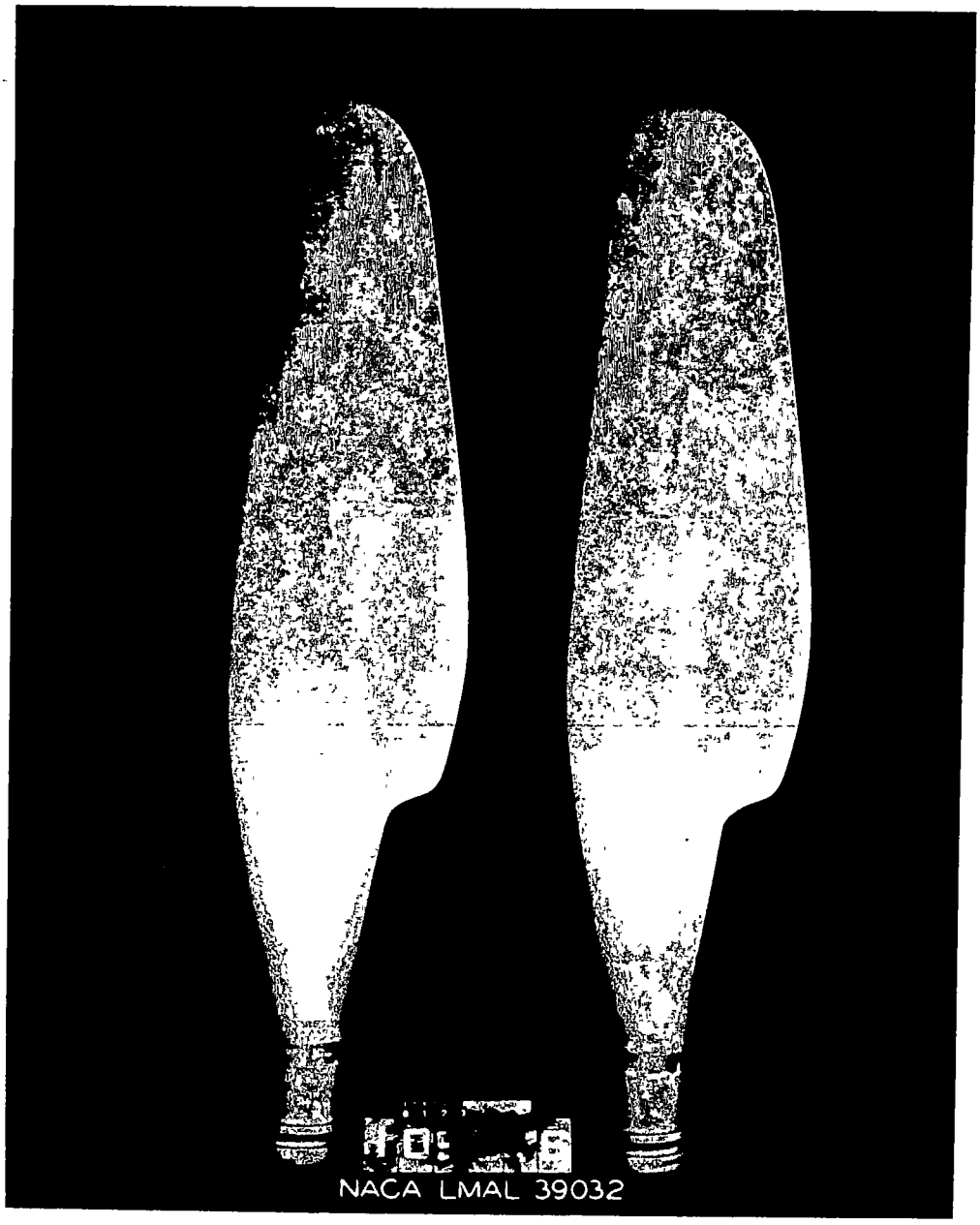

Figure 9.- Propeller blades 109376 (40-percent trailing-edge extension) - cambered face (upper surface).

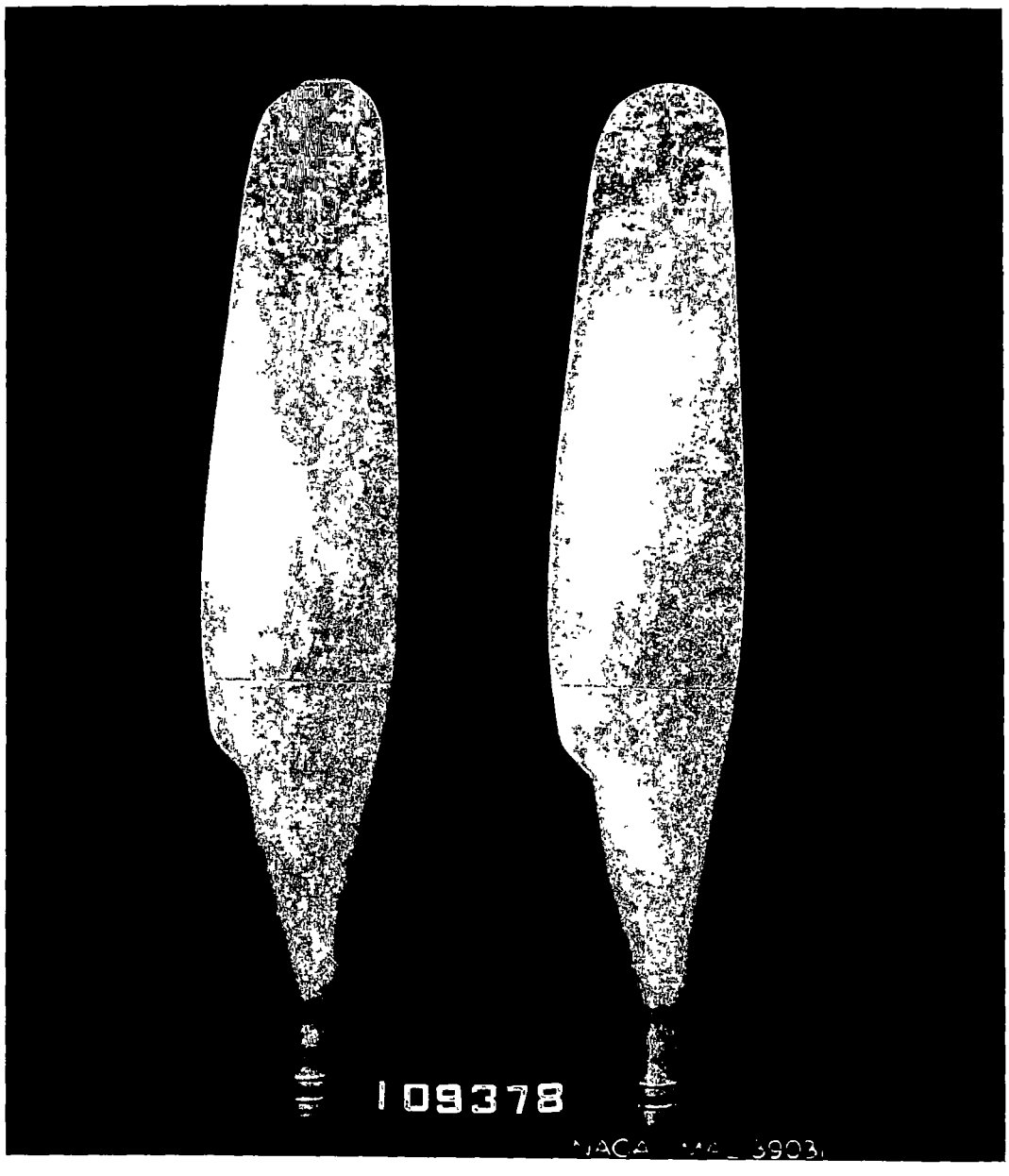

Figure 10.- Propeller blades 109378 (20-percent trailing-edge extension) - thrust face (lower surface).

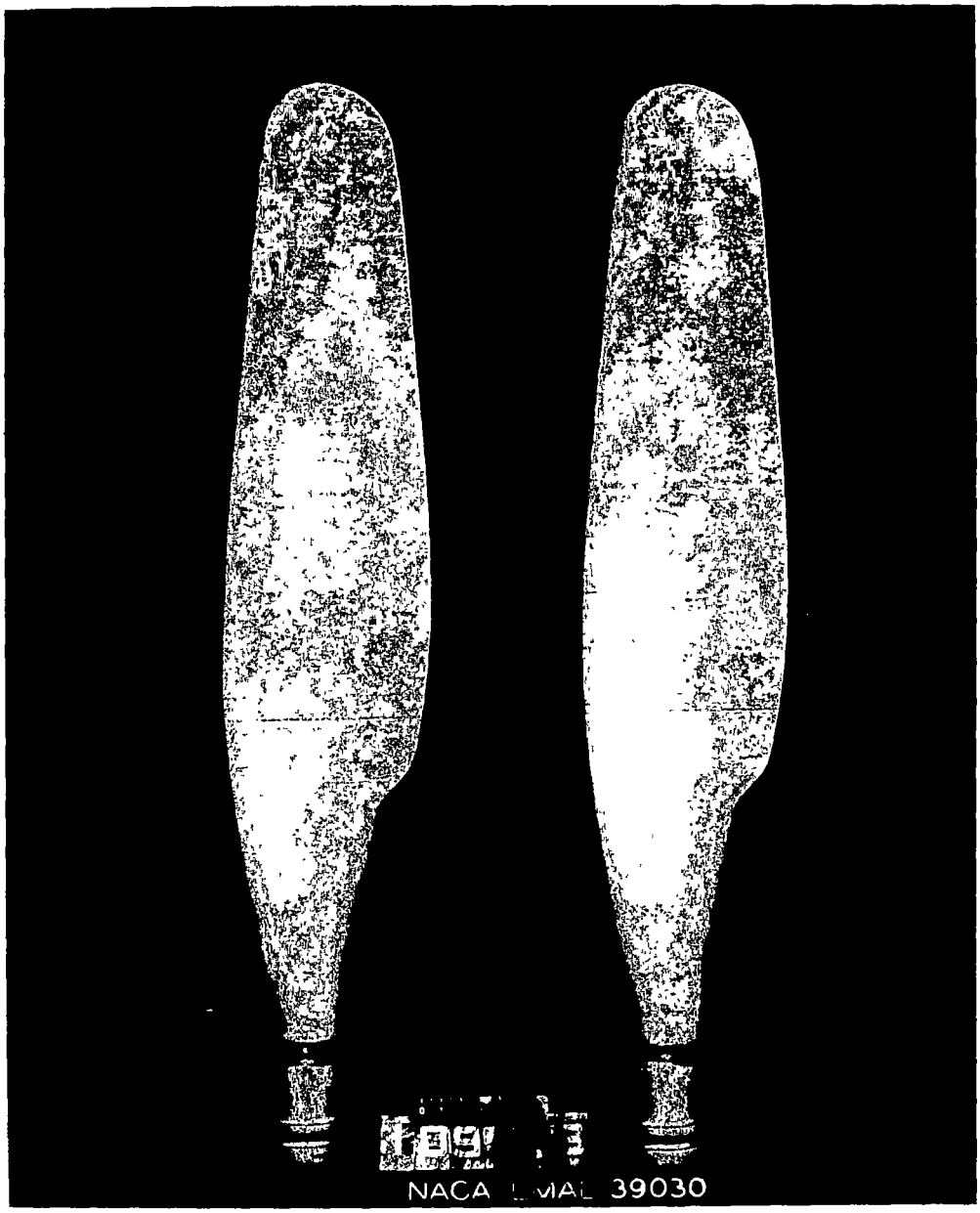

Figure 11.- Propeller blades 109378 (20-percent trailing-edge extension) - cambered face (upper surface).

Figure 12.- Propeller blades 109376-modified (original 40-percent trailing-edge extension cut to form a 20-percent extension) - thrust face (lower surface).

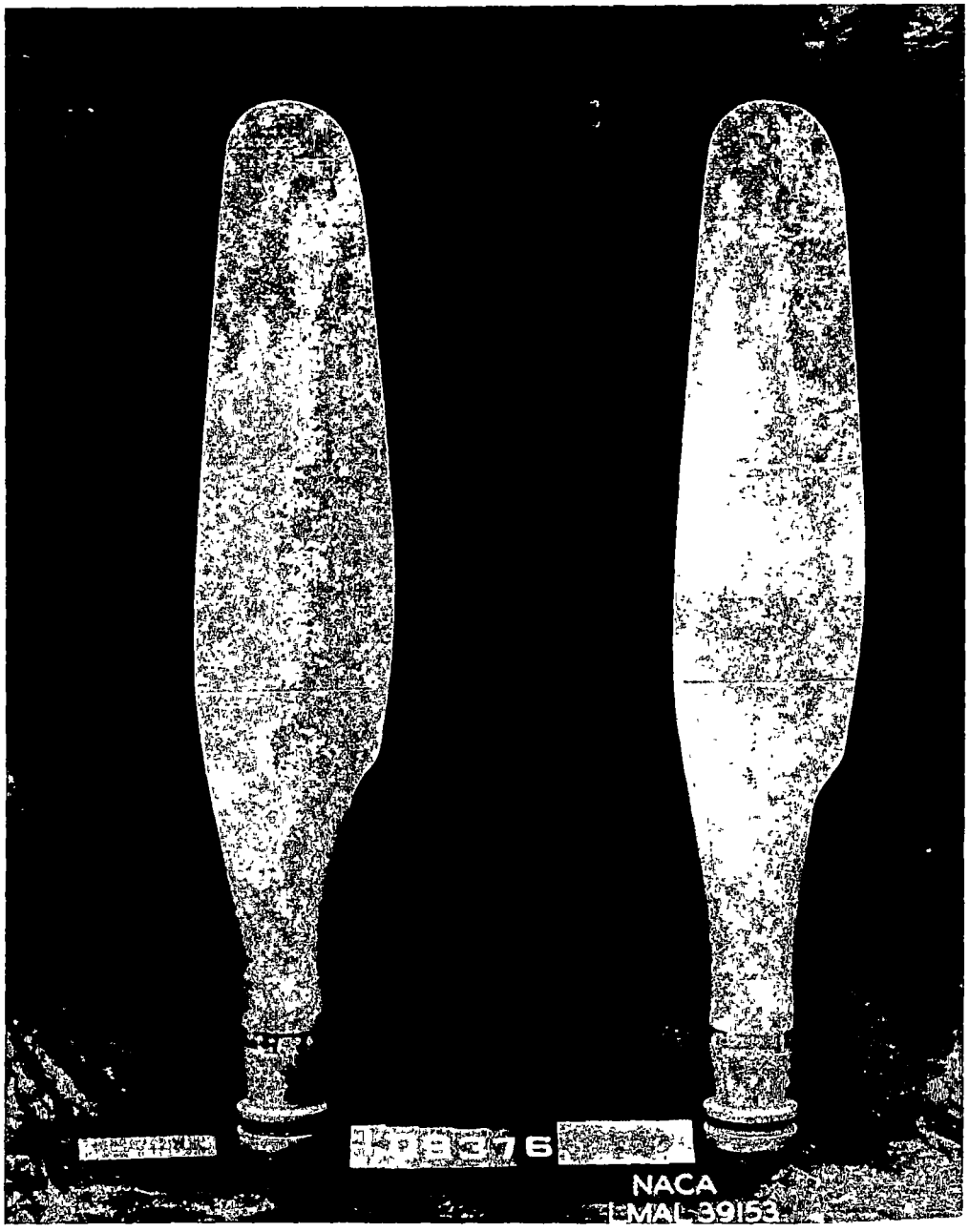

Figure 13.- Propeller blades 109376-modified (original 40-percent trailing-edge extension cut to form a 20-percent extension) - cambered face (upper surface).

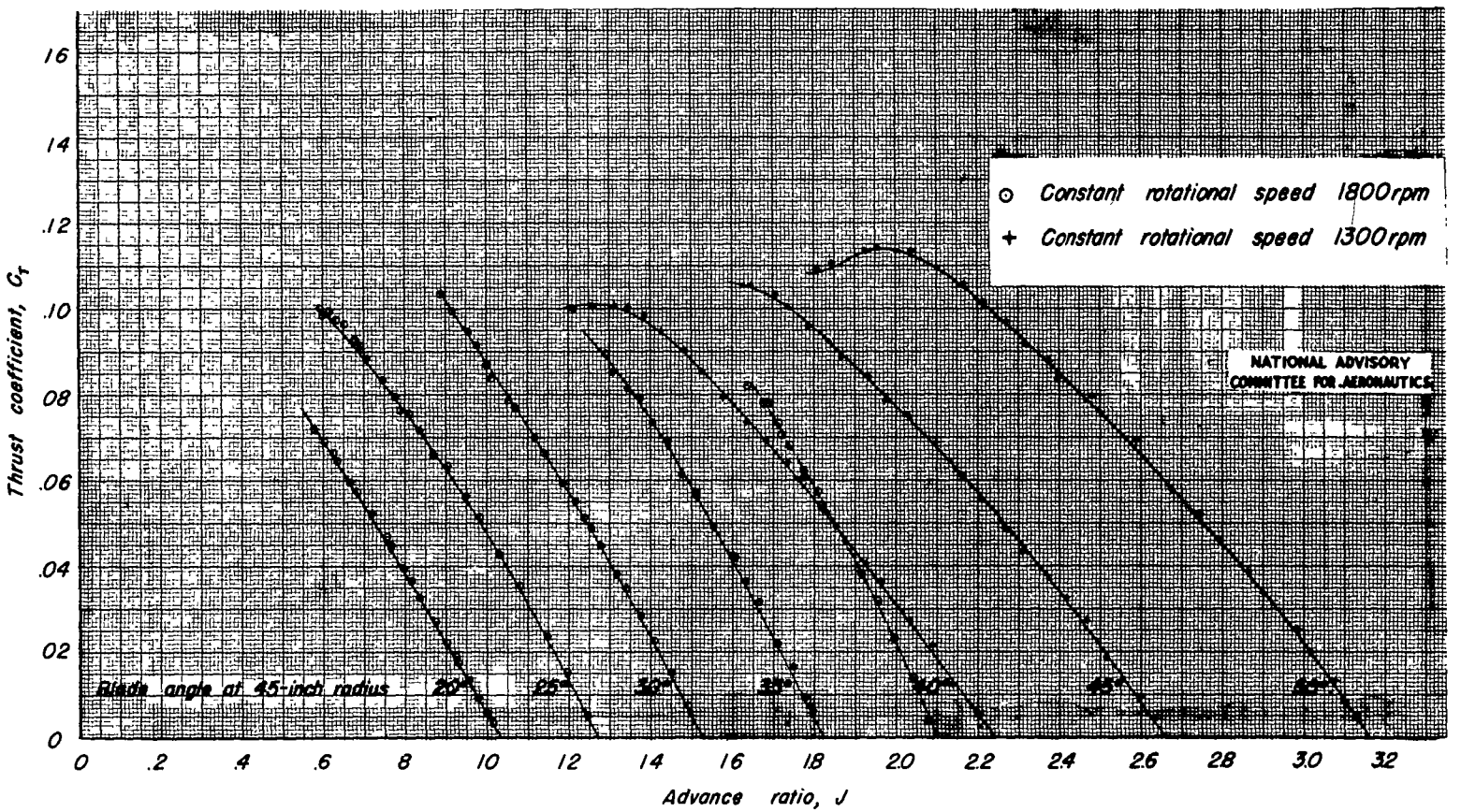

Figure 14.—Variation of thrust coefficient with advance ratio, propeller 109374, no trailing edge extension.

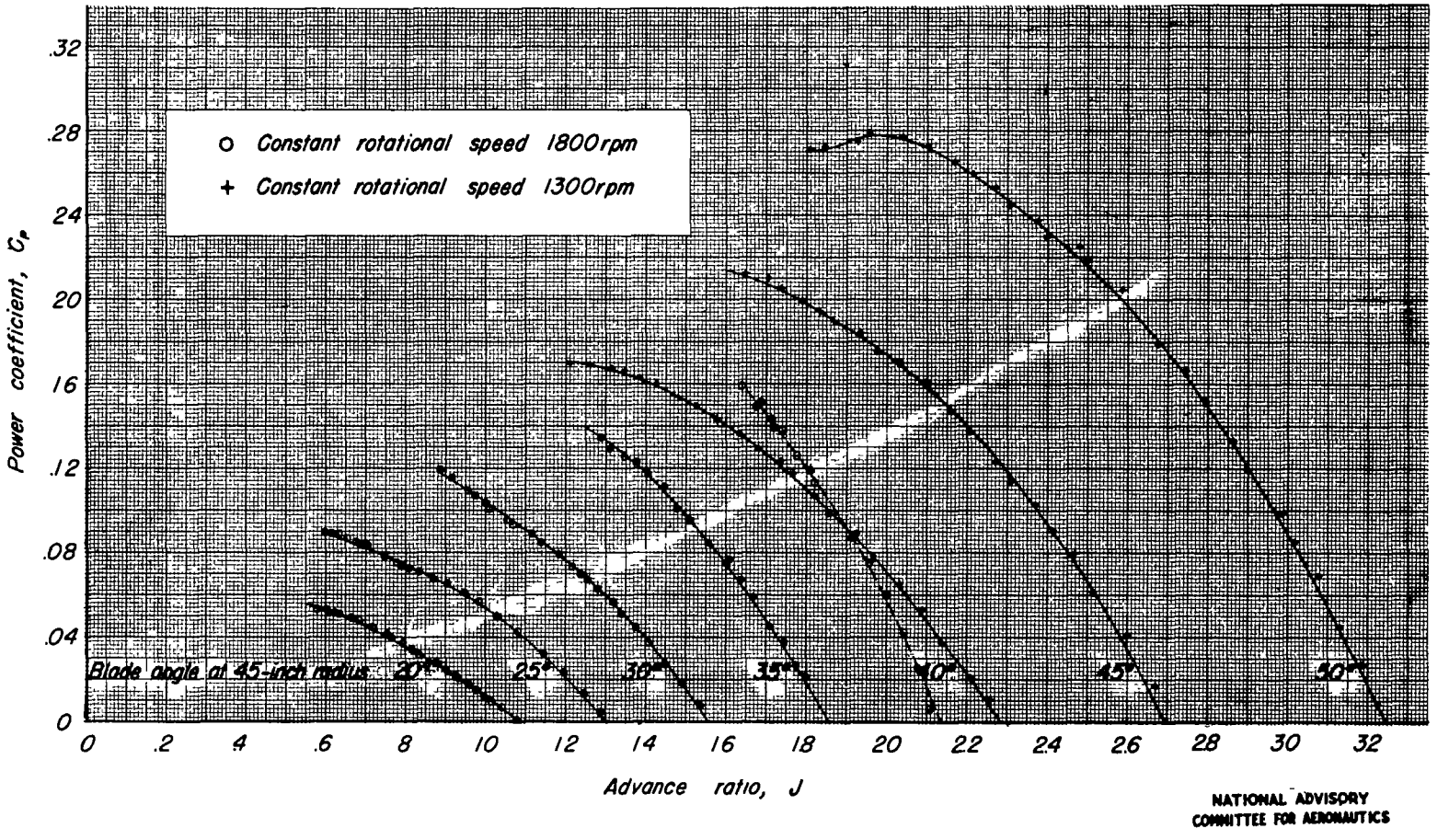

Figure 15.—Variation of power coefficient with advance ratio, propeller 109374, no trailing edge extension.

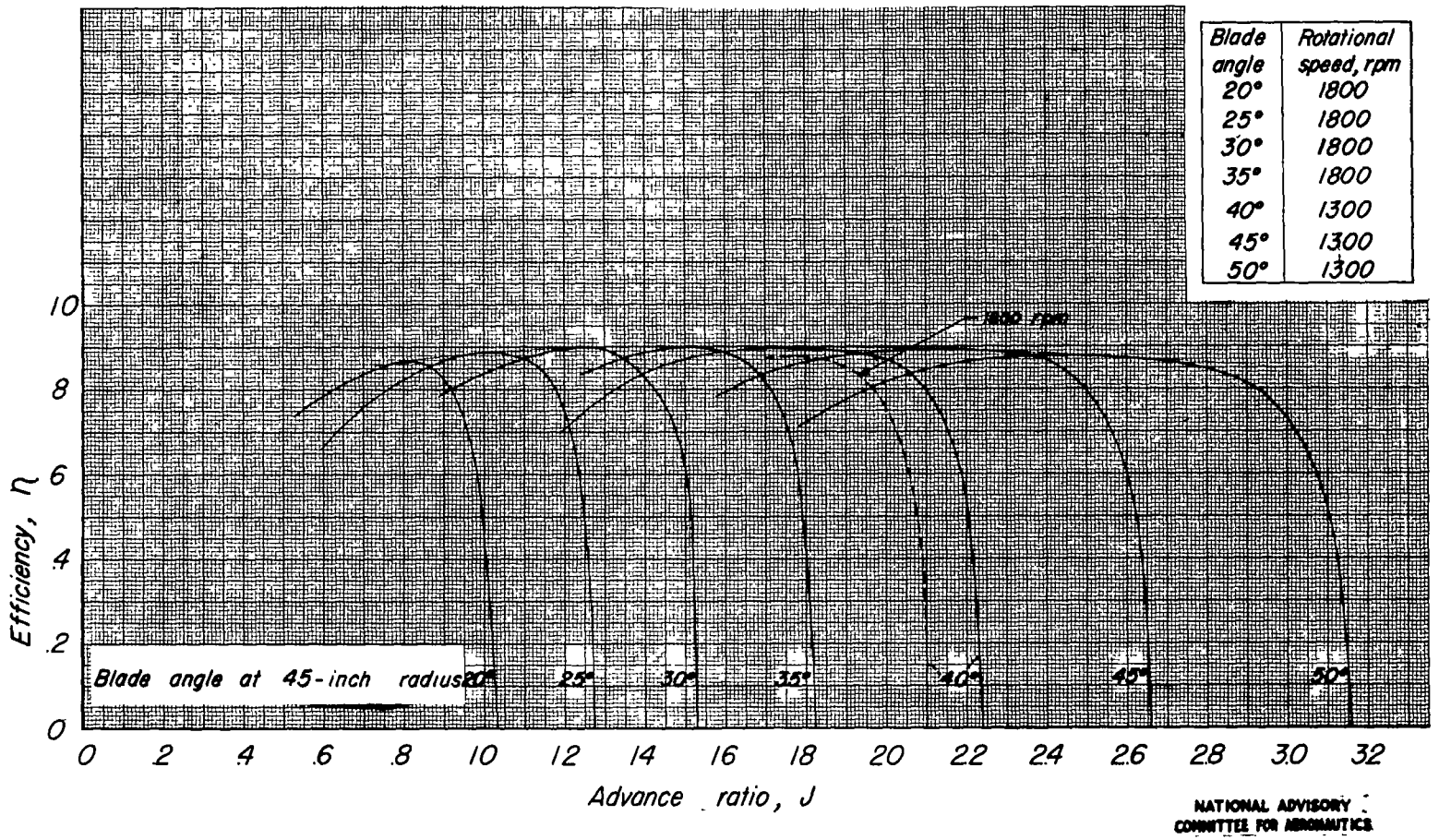

Figure 16.—Variation of propeller efficiency with advance ratio, propeller 109374, no trailing-edge extension.

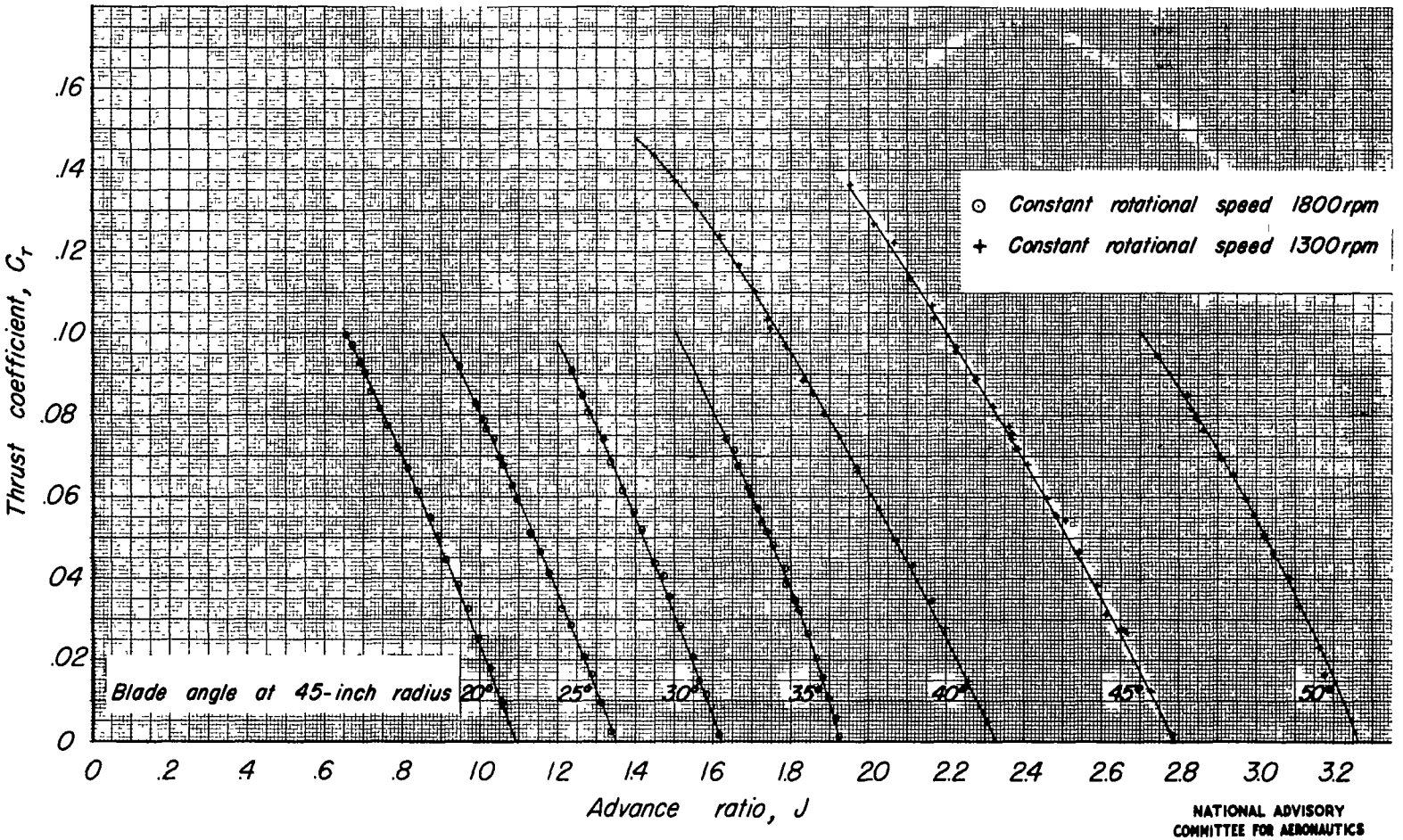

Figure 17.—Variation of thrust coefficient with advance ratio, propeller 109376, 40 percent trailing edge extension.

MR No. L5G10

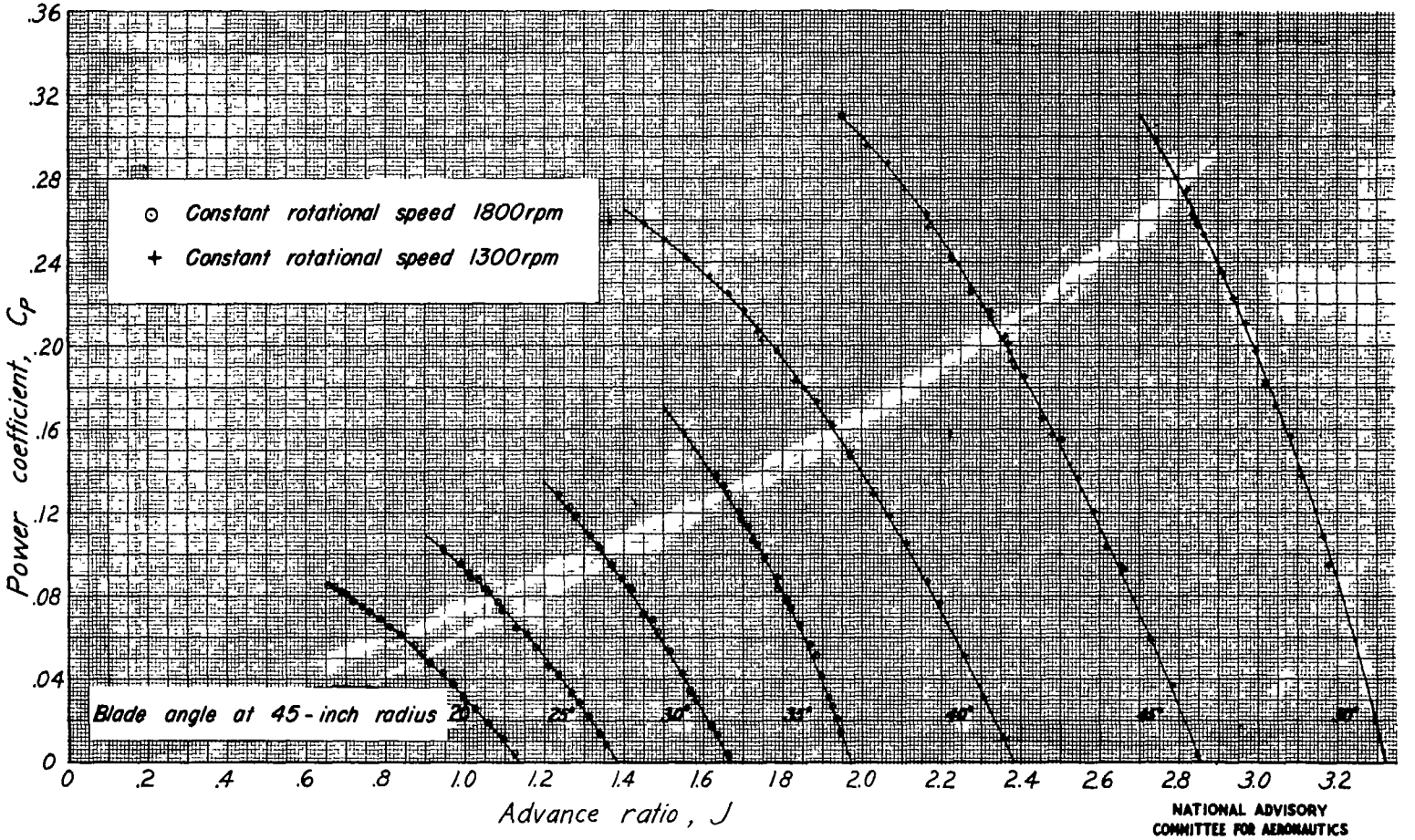

Figure 18.—Variation of power coefficient with advance ratio, propeller 109376, 40 percent trailing edge extension.

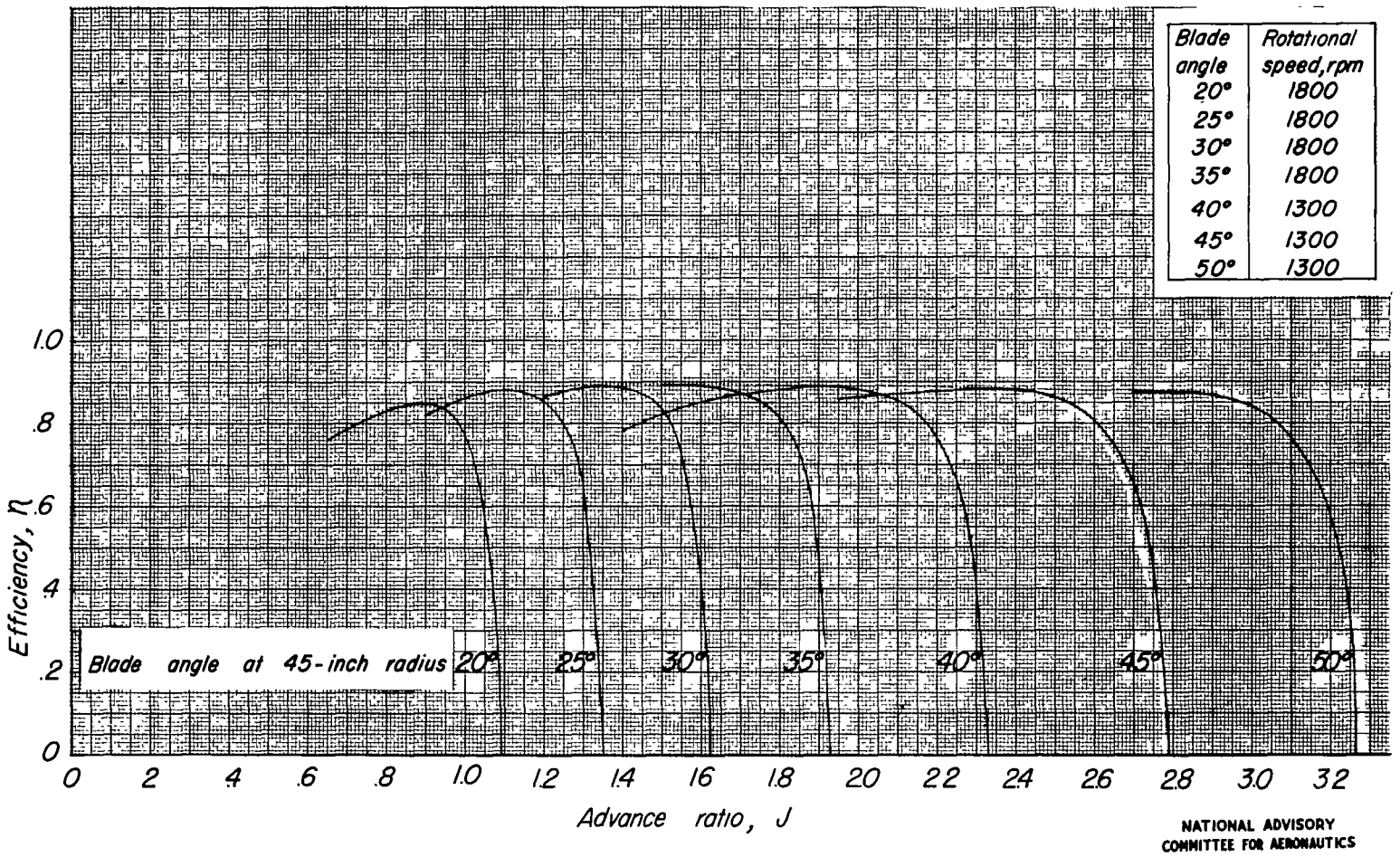

Figure 19.—Variation of propeller efficiency with advance ratio, propeller 109376, 40% trailing edge extension.

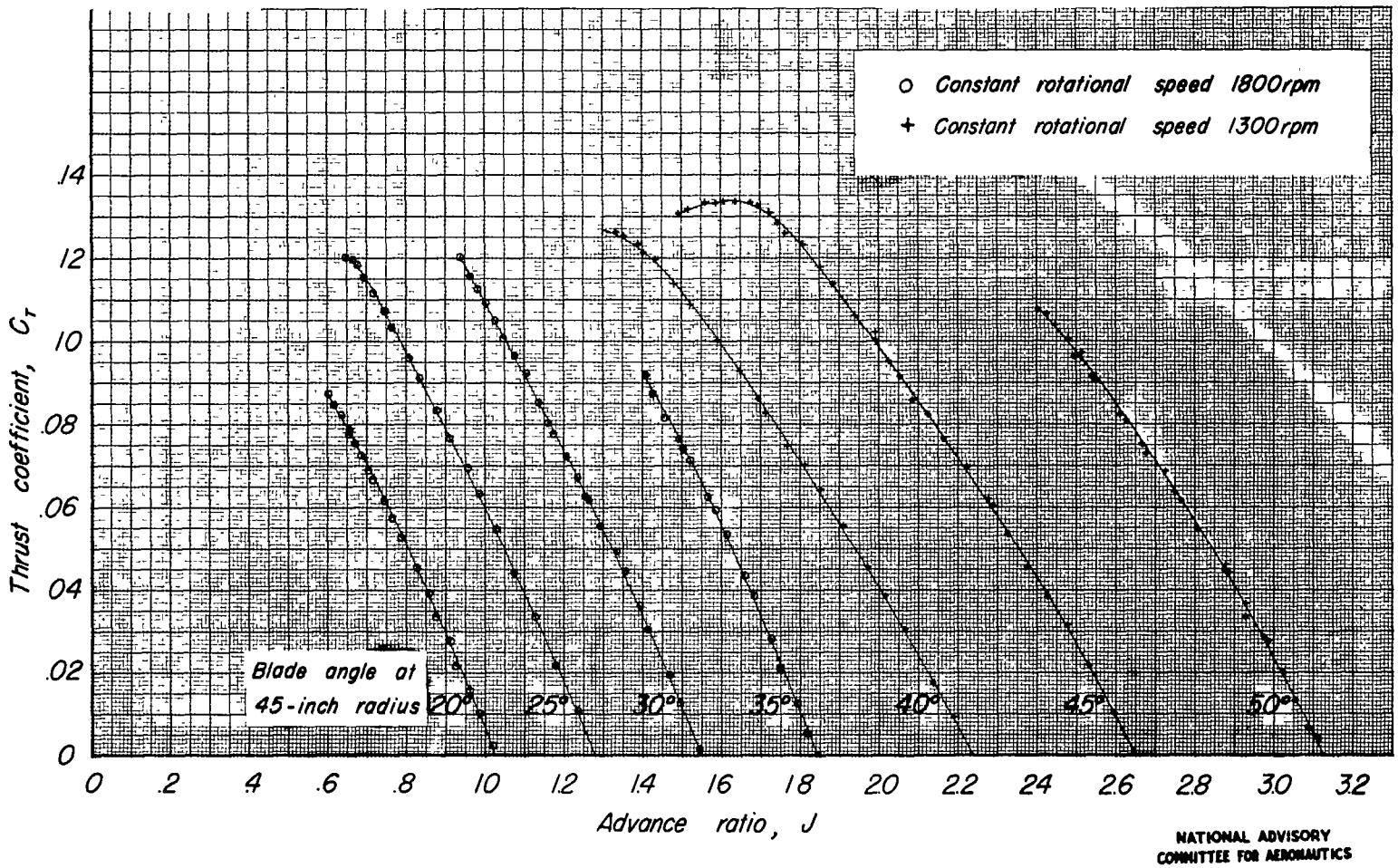

Figure 20.—Variation of thrust coefficient with advance ratio, propeller 109378, 20 percent trailing edge extension.

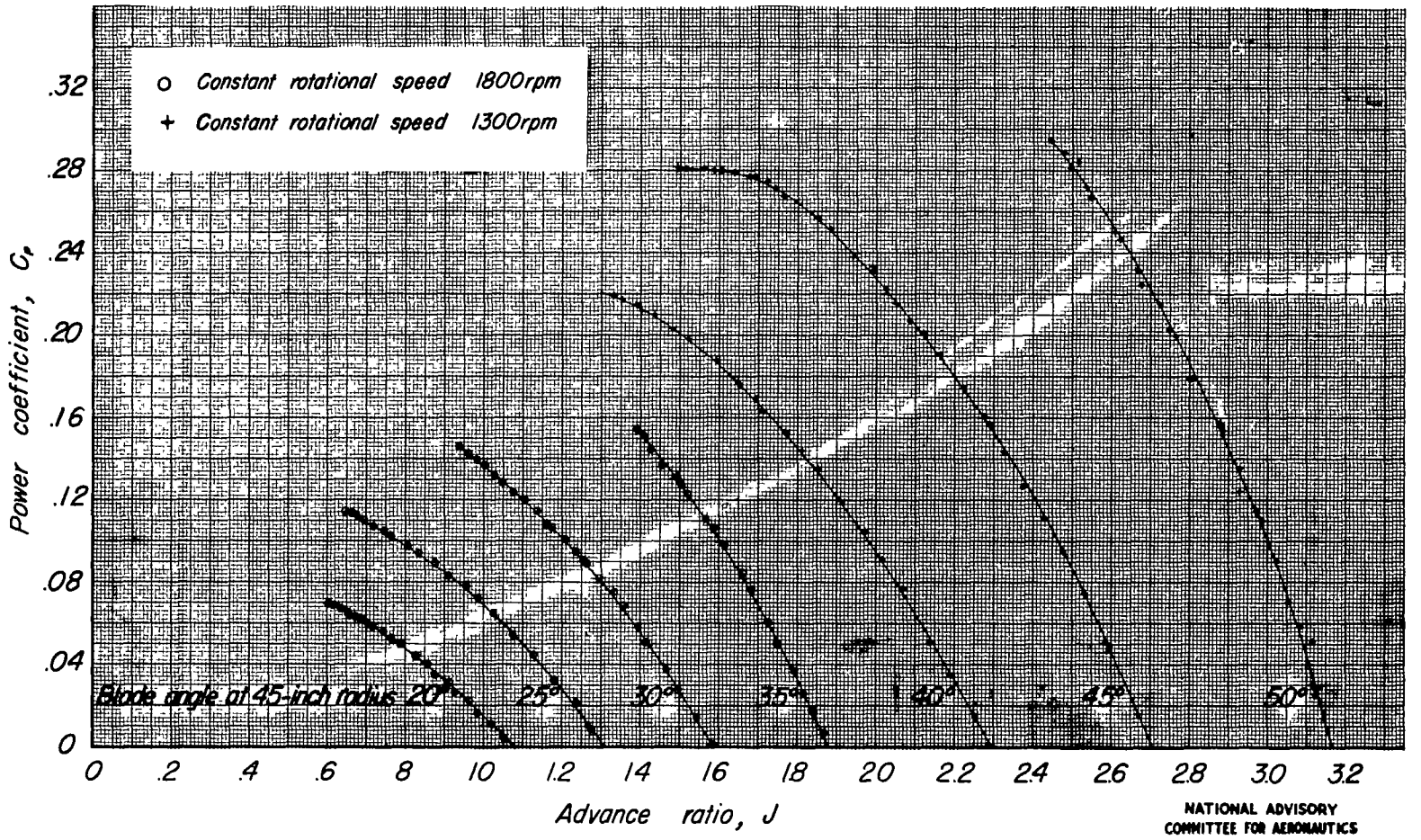

Figure 21.—Variation of power coefficient with advance ratio, propeller 109378, 20 percent trailing edge extension.

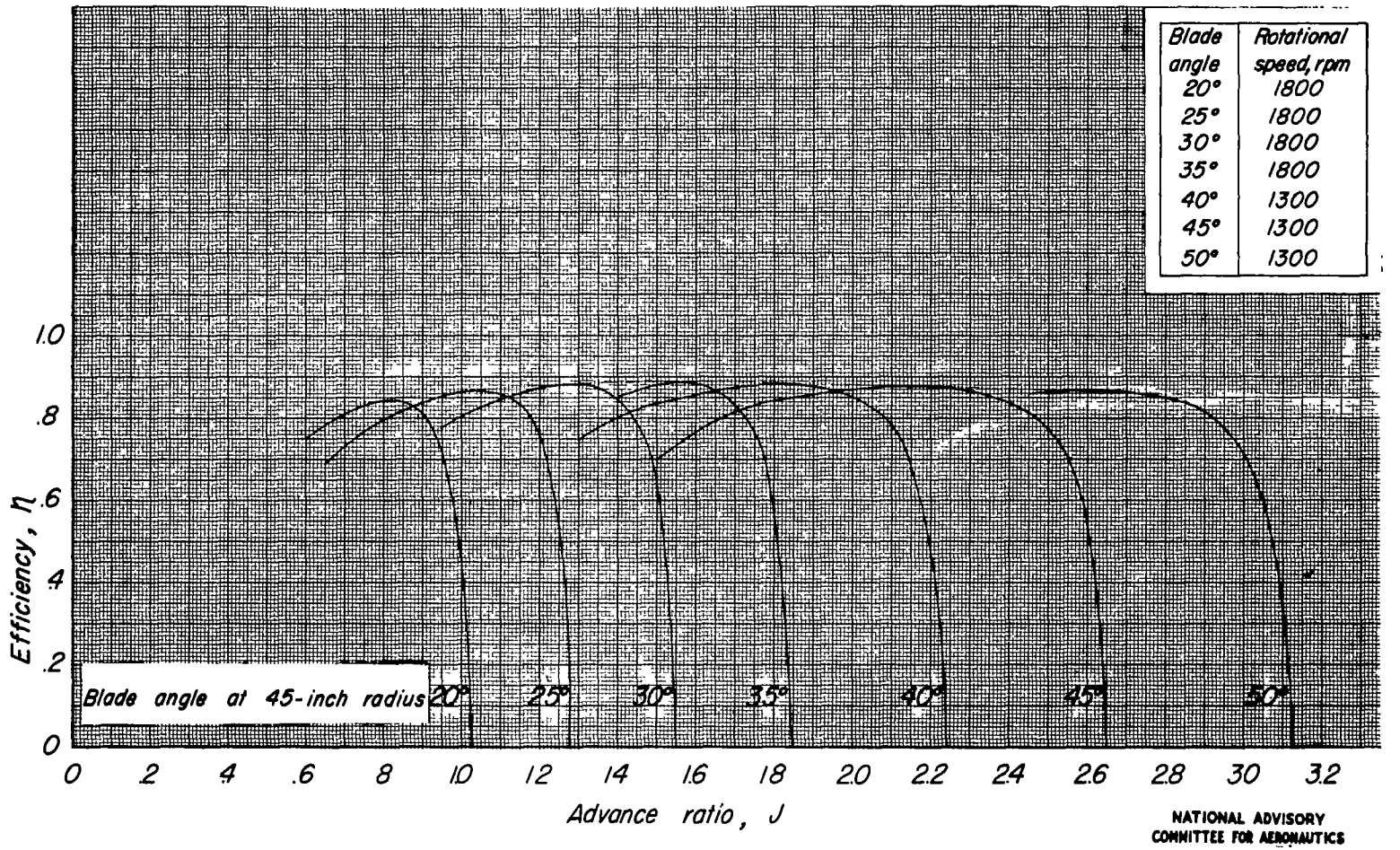

Figure 22.—Variation of propeller efficiency with advance ratio, propeller 109378, 20 percent trailing edge extension.

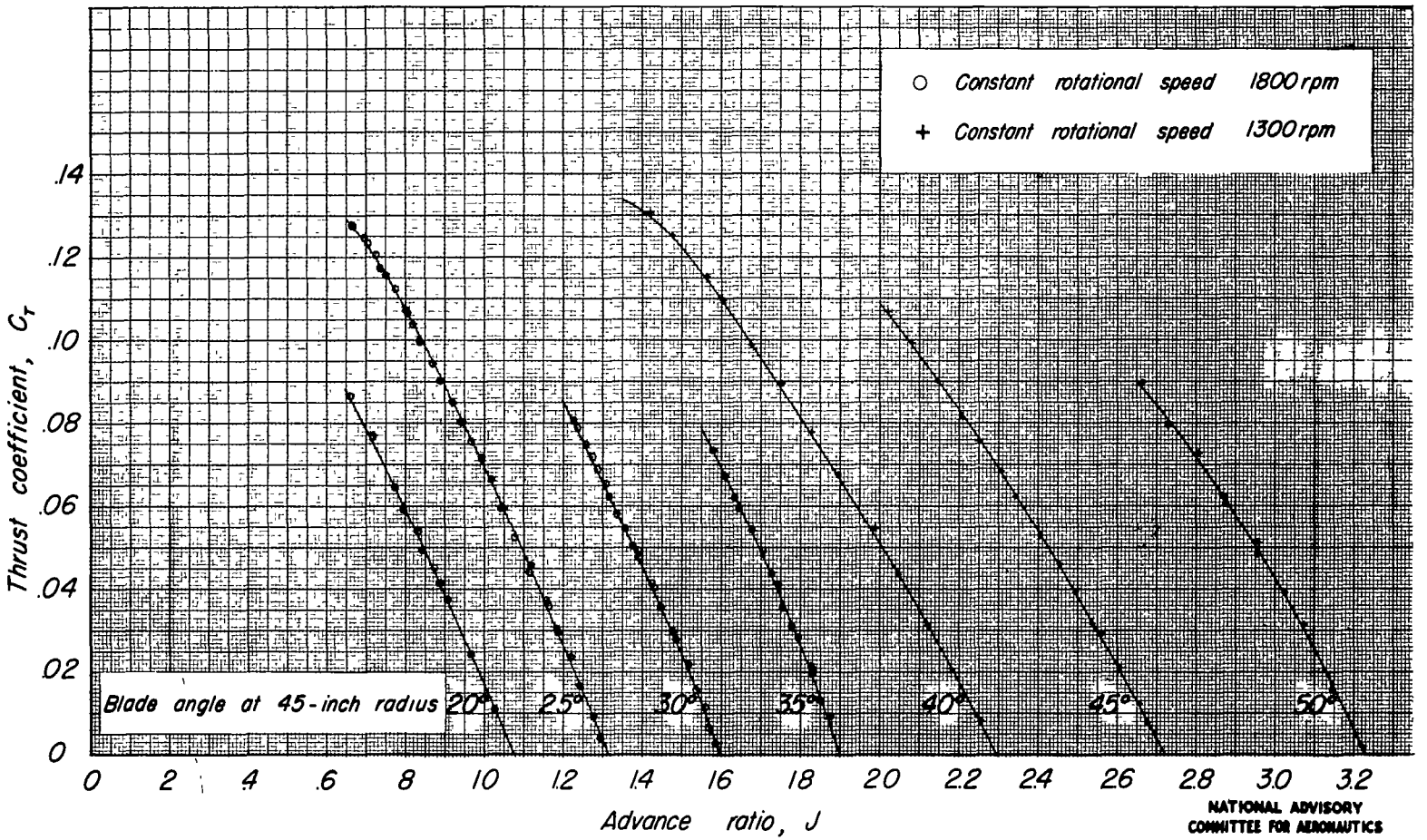

Figure 23.—Variation of thrust coefficient with advance ratio, propeller 109376-modified, original trailing edge extension cut to form a 20 percent extension.

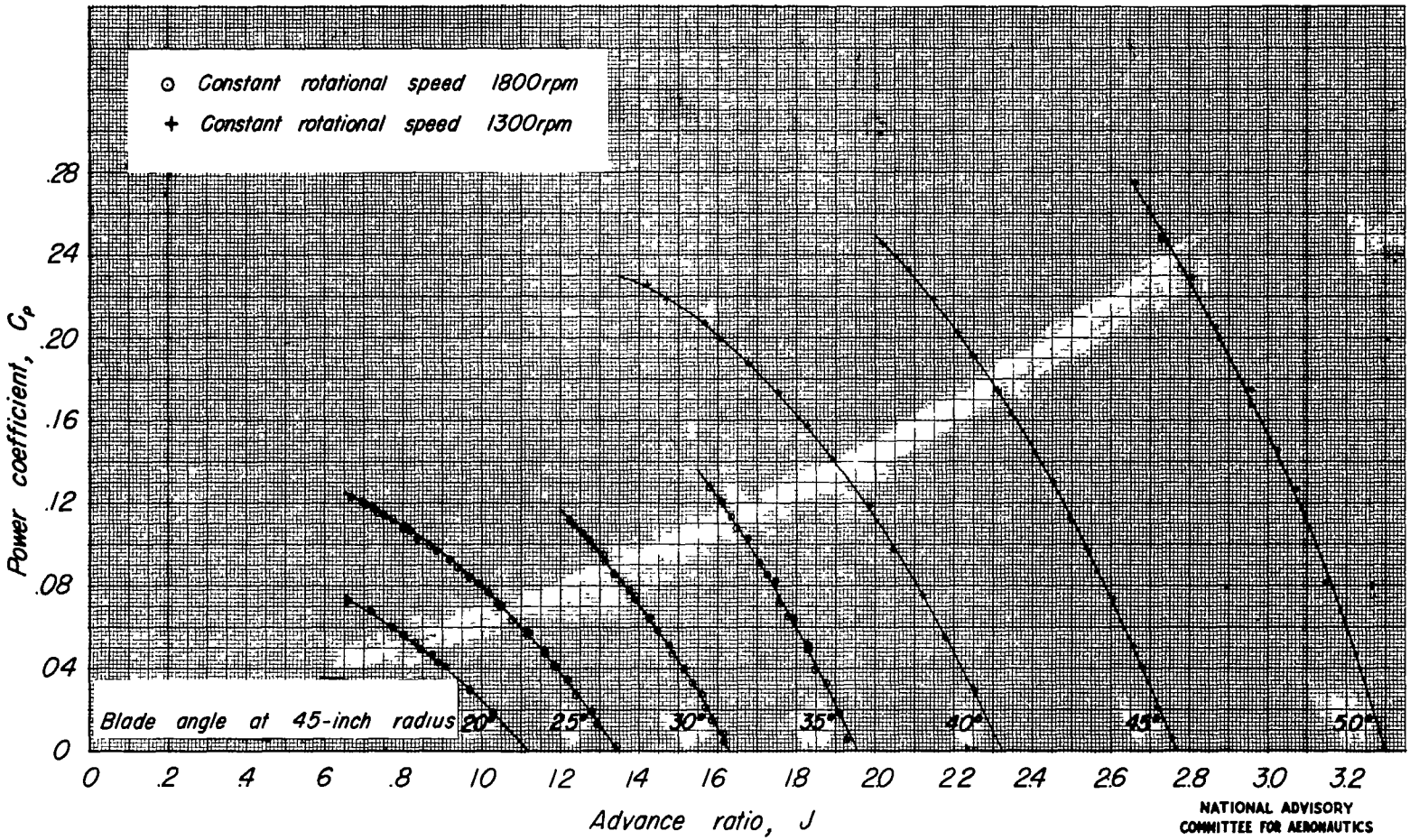

Figure 24.—Variation of power coefficient with advance ratio, propeller 109376-modified, original trailing edge cut to form a 20 percent extension

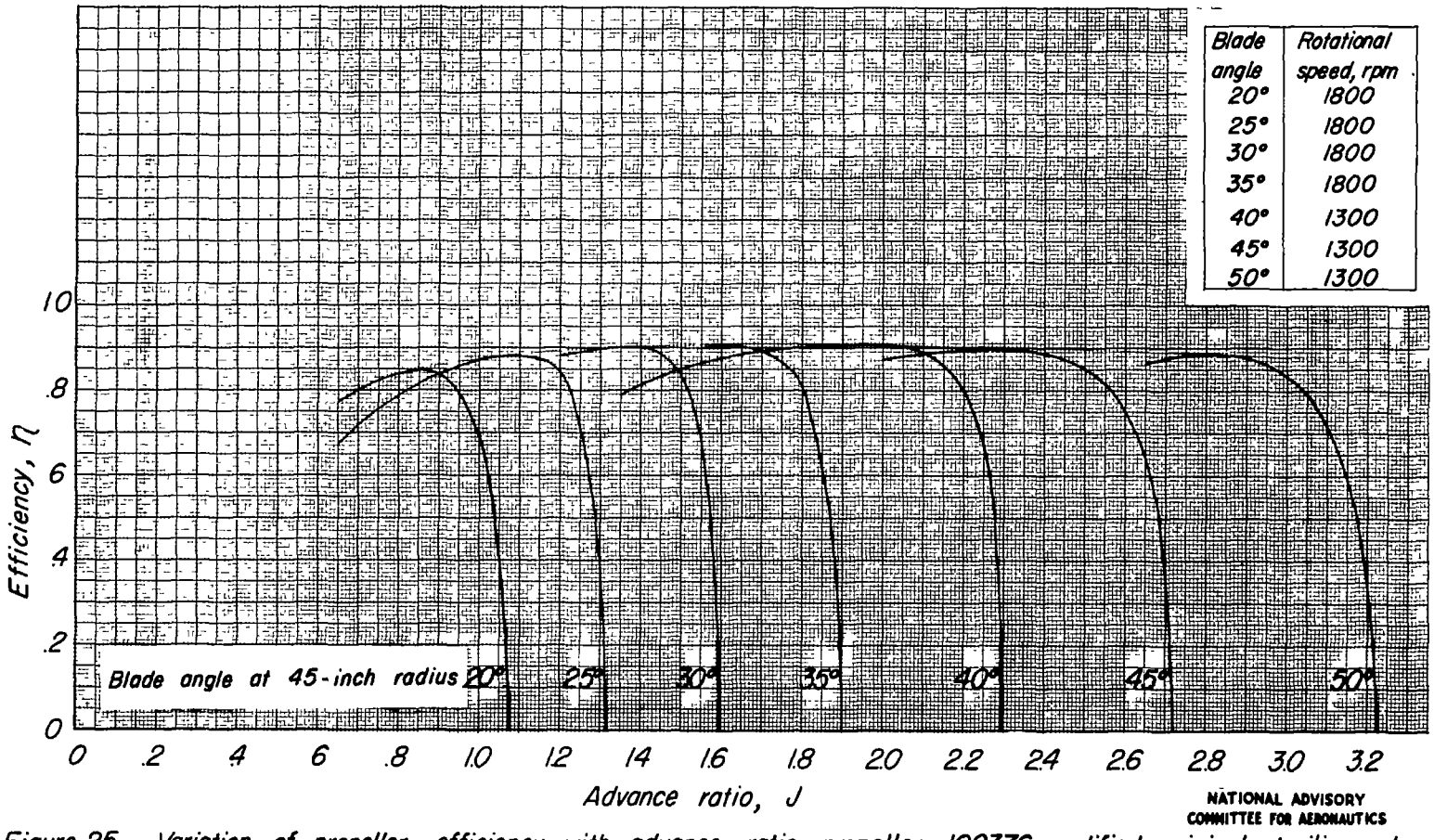

Figure 25.—Variation of propeller efficiency with advance ratio, propeller 109376-modified, original trailing edge extension cut to form a 20 percent extension.

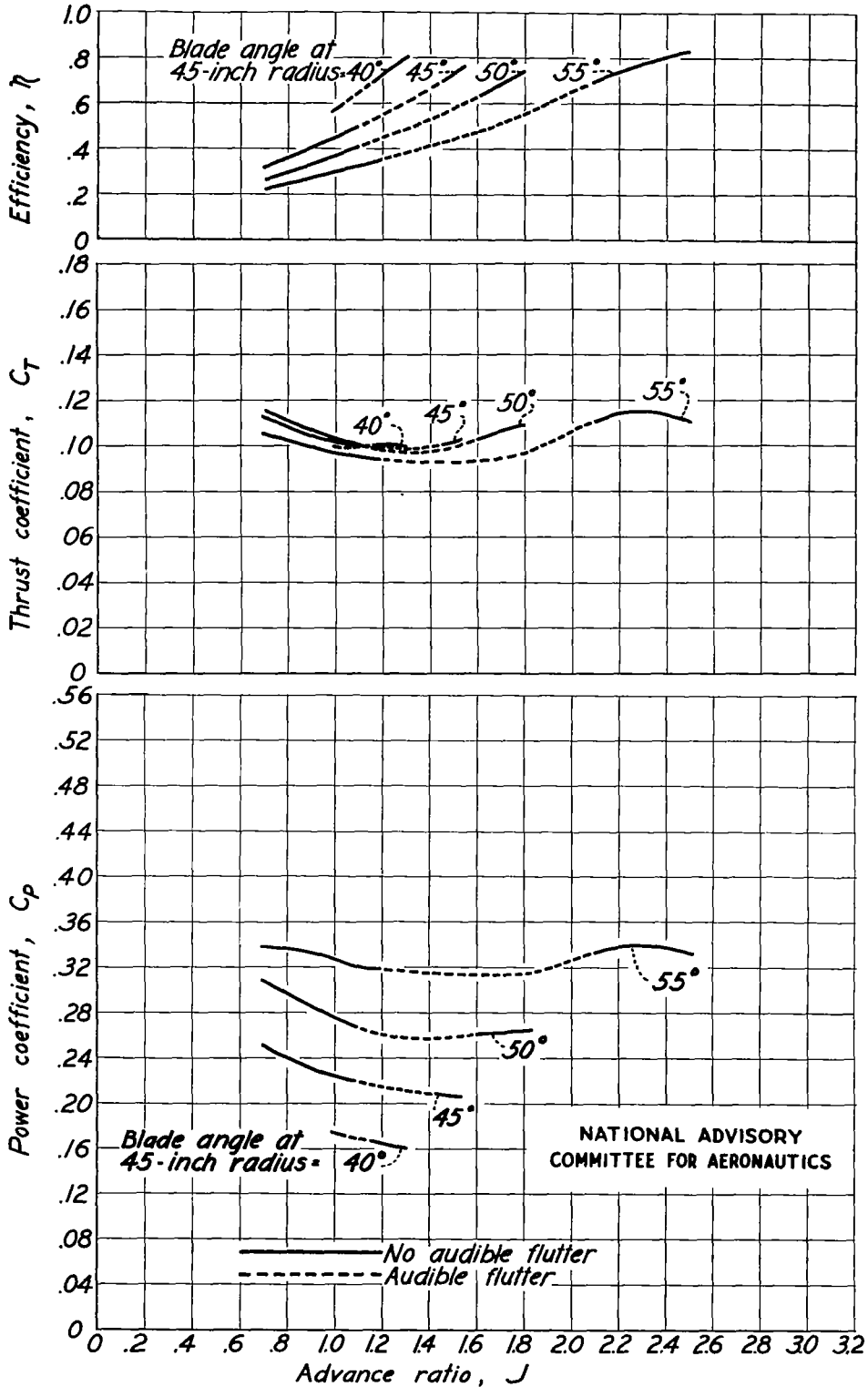

Figure 26.—Propeller characteristics in the region of stalled flutter for propeller 109374, no trailing edge extension, constant rotational speed 1000 rpm.

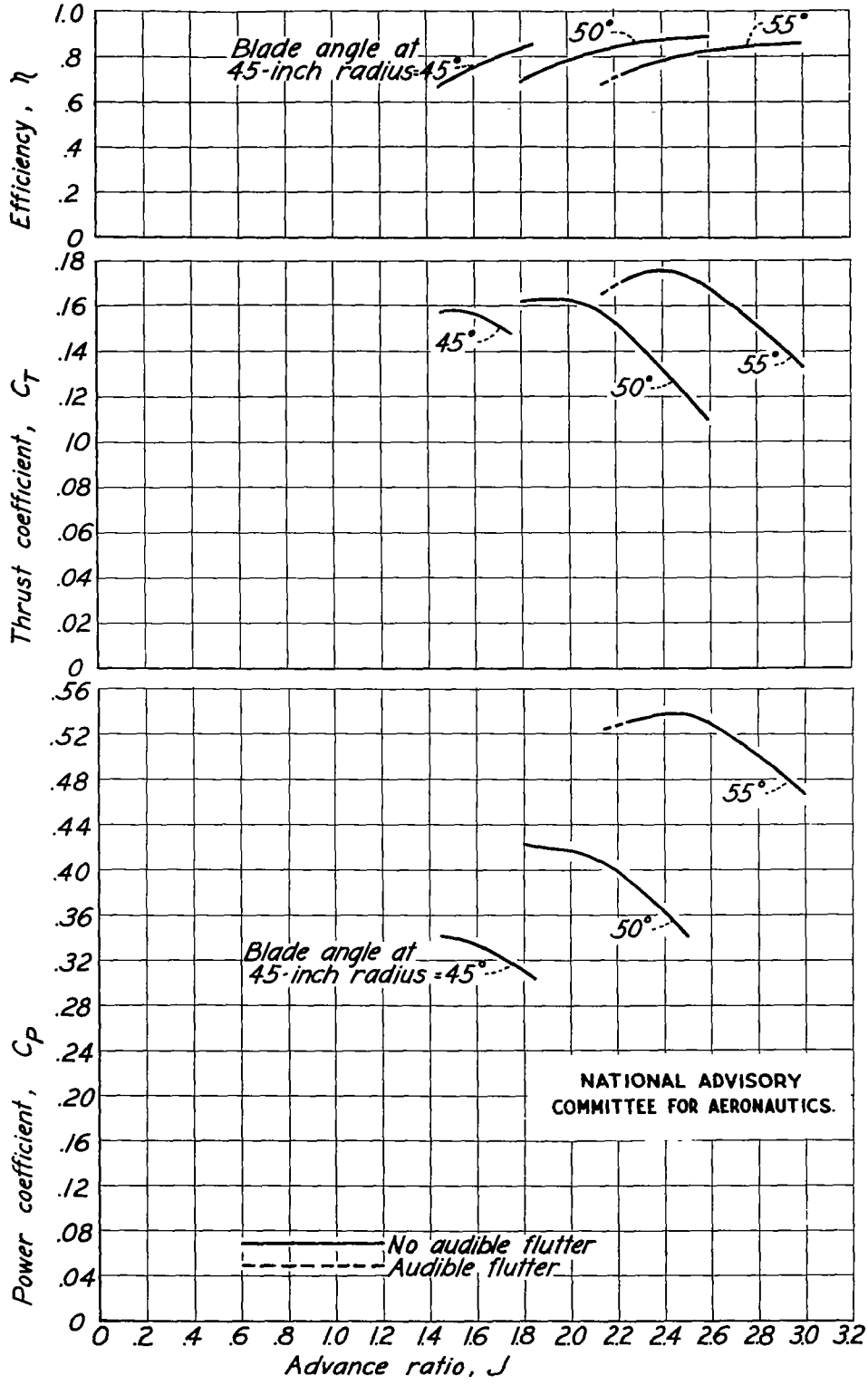

Figure 27.—Propeller characteristics in the region of stalled flutter for propeller 109376, 40 percent trailing edge extension, constant rotational speed 1000 rpm.

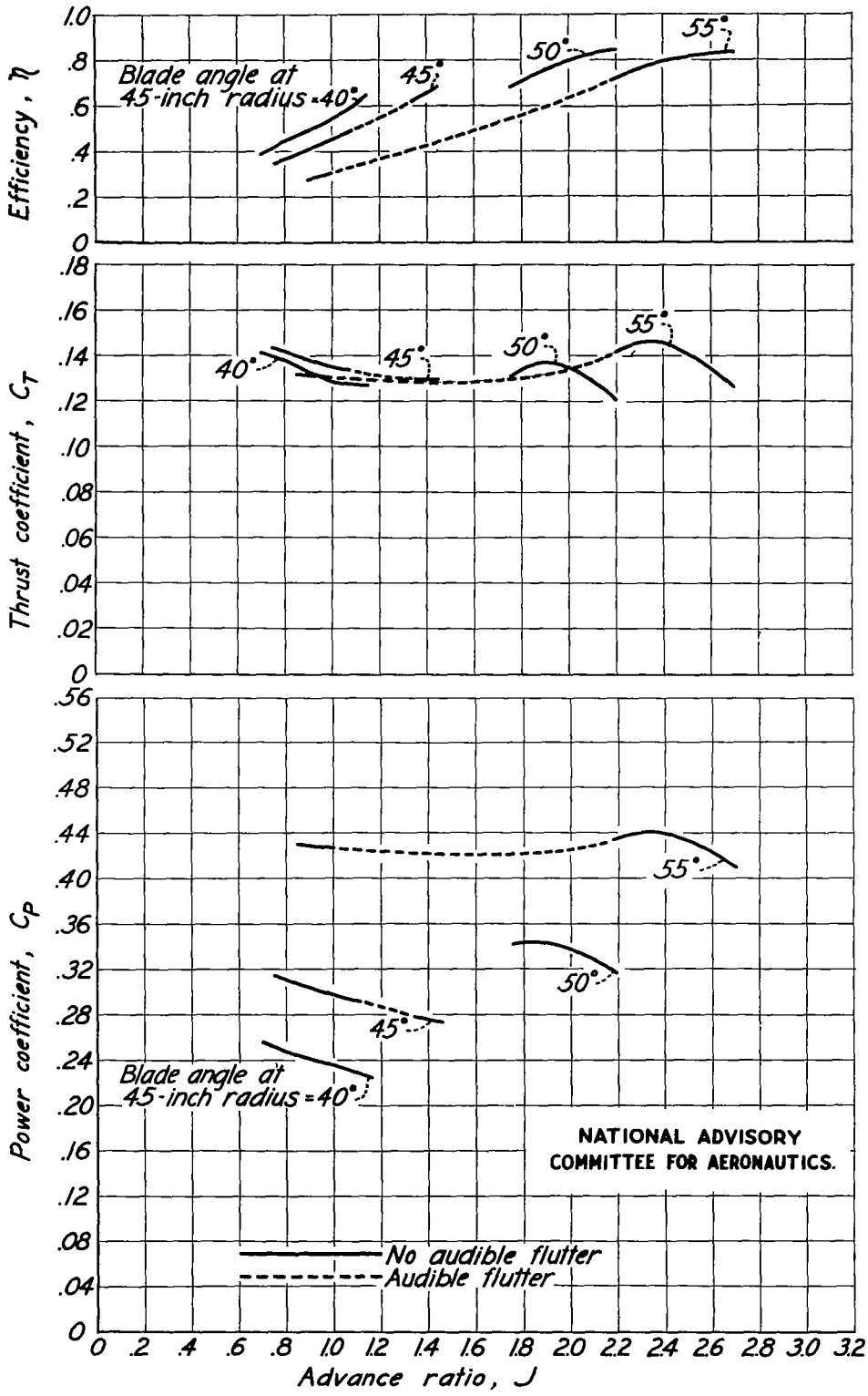

Figure 28.—Propeller characteristics in the region of stalled flutter for propeller 109378, 20 percent trailing edge extension, constant rotational speed 1000 rpm.

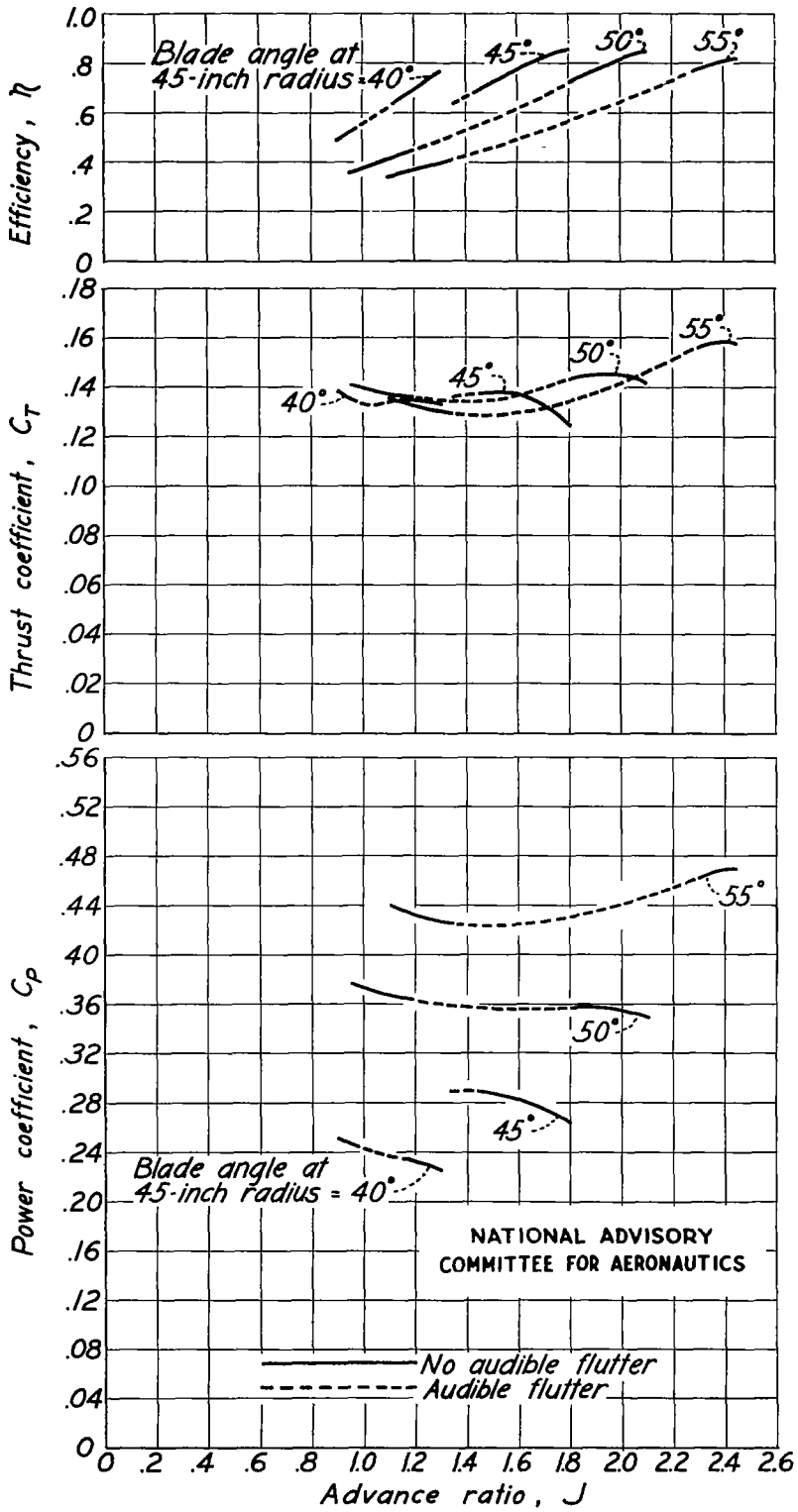

Figure 29.—Propeller characteristics in the region of stalled flutter for propeller 109376 modified, original trailing edge extension cut to form a 20 percent extension, constant rotational speed 1000 rpm.

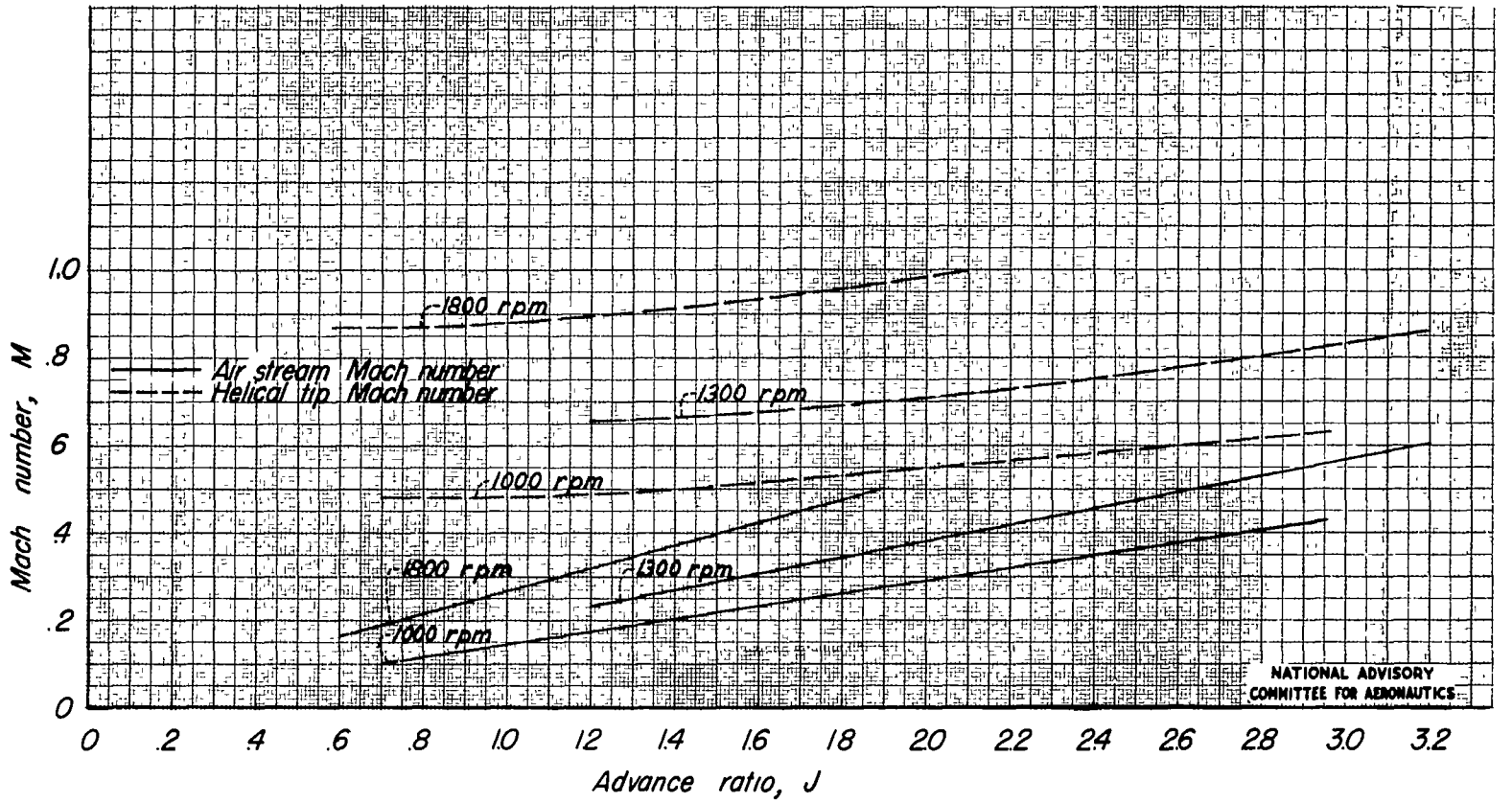

Figure 30.—Variation of air stream Mach number and helical tip Mach number with advance ratio.

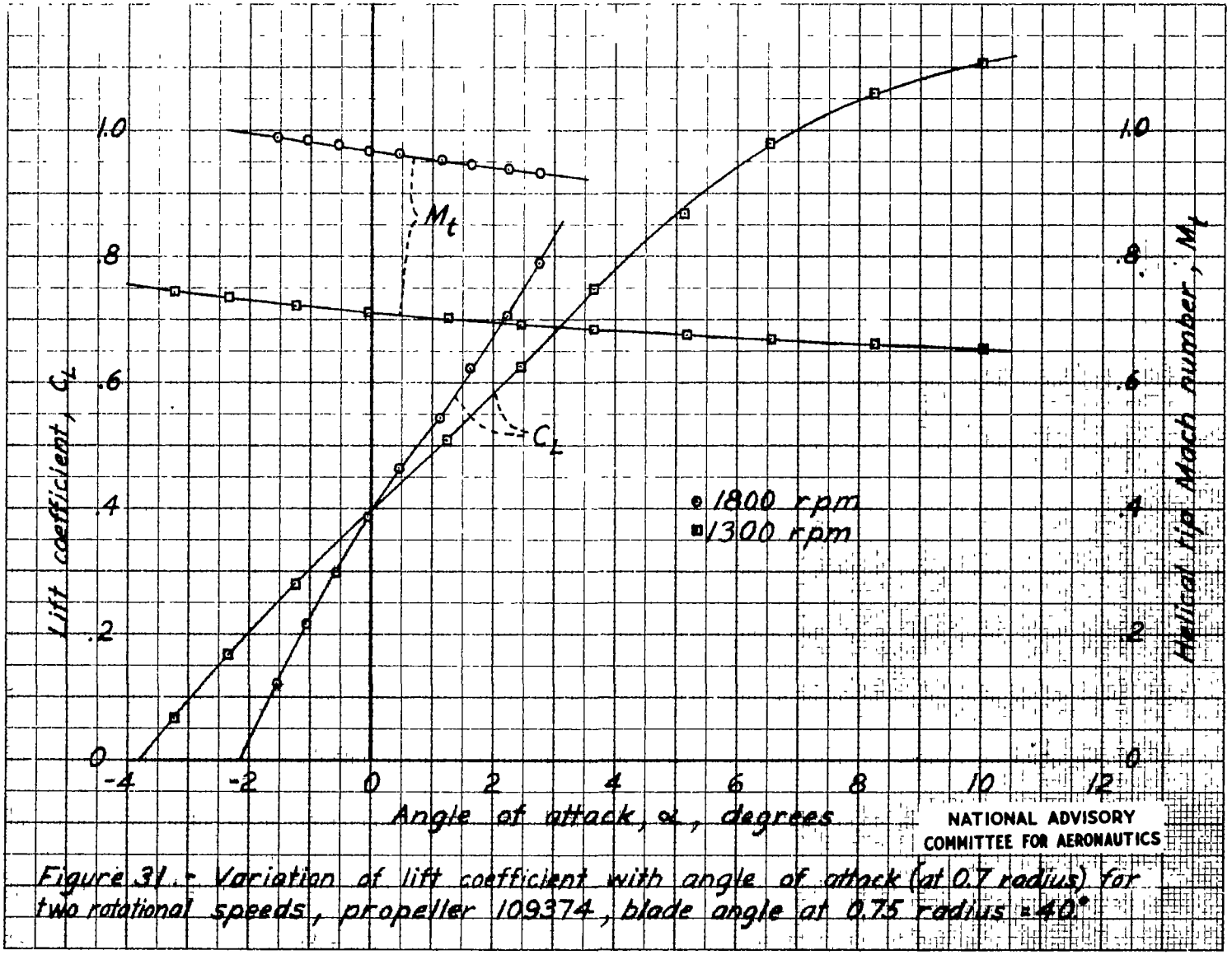

Figure 31.- Variation of lift coefficient with angle of attack (at 0.7 radius) for two rotational speeds, propeller 109374, blade angle at 0.75 radius = 40°.

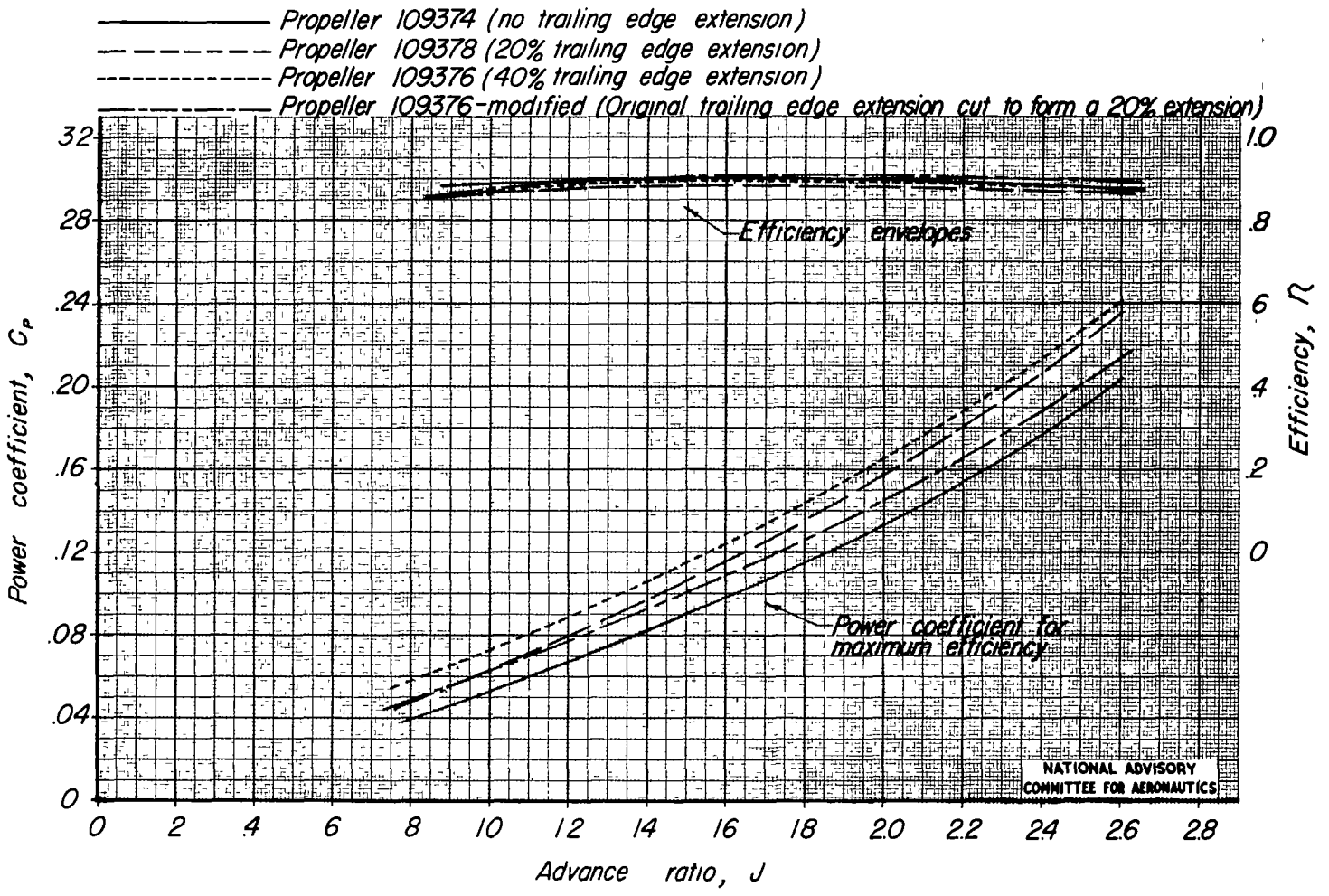

Figure 32 — Envelope curves of propeller efficiency and power coefficient for maximum efficiency for the four propellers tested.

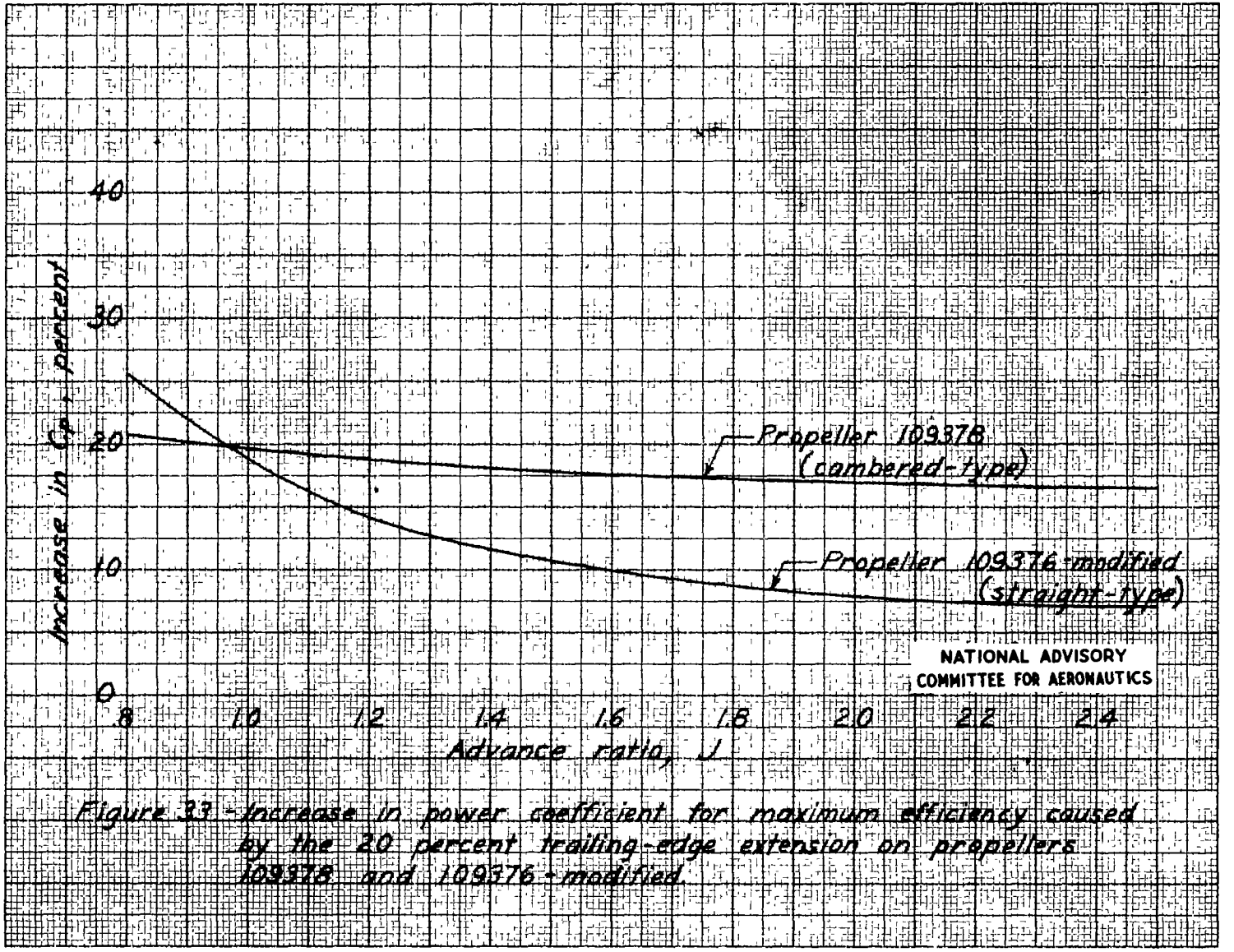

Figure 33 - Increase in power coefficient for maximum efficiency caused by the 20 percent trailing-edge extension on propellers 109376 and 109376-modified.

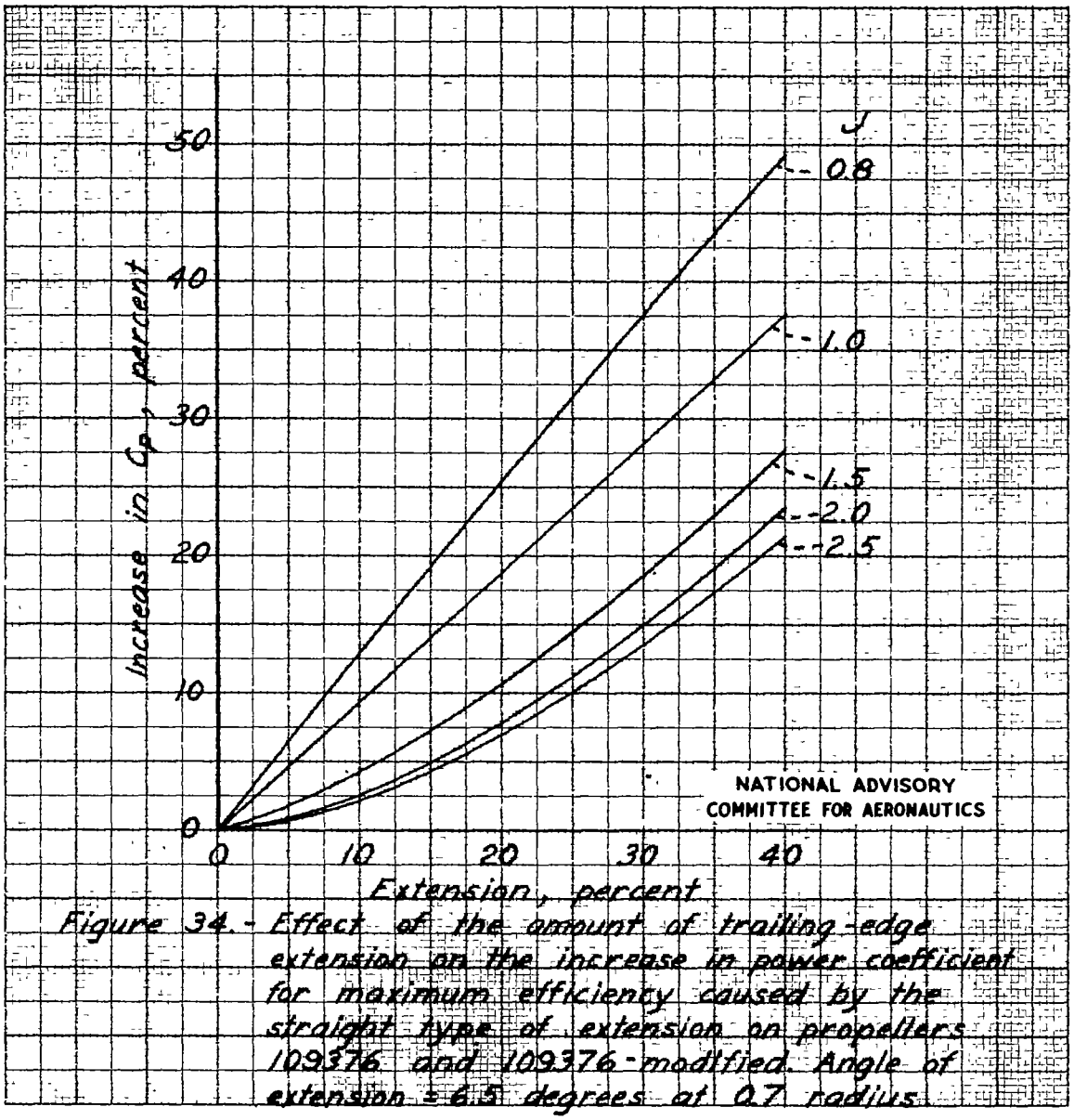

Figure 34.- Effect of the amount of trailing-edge extension on the increase in power coefficient for maximum efficiency caused by the straight type of extension on propellers 109376 and 109376-modified. Angle of extension = 6.5 degrees at 0.7 radius.

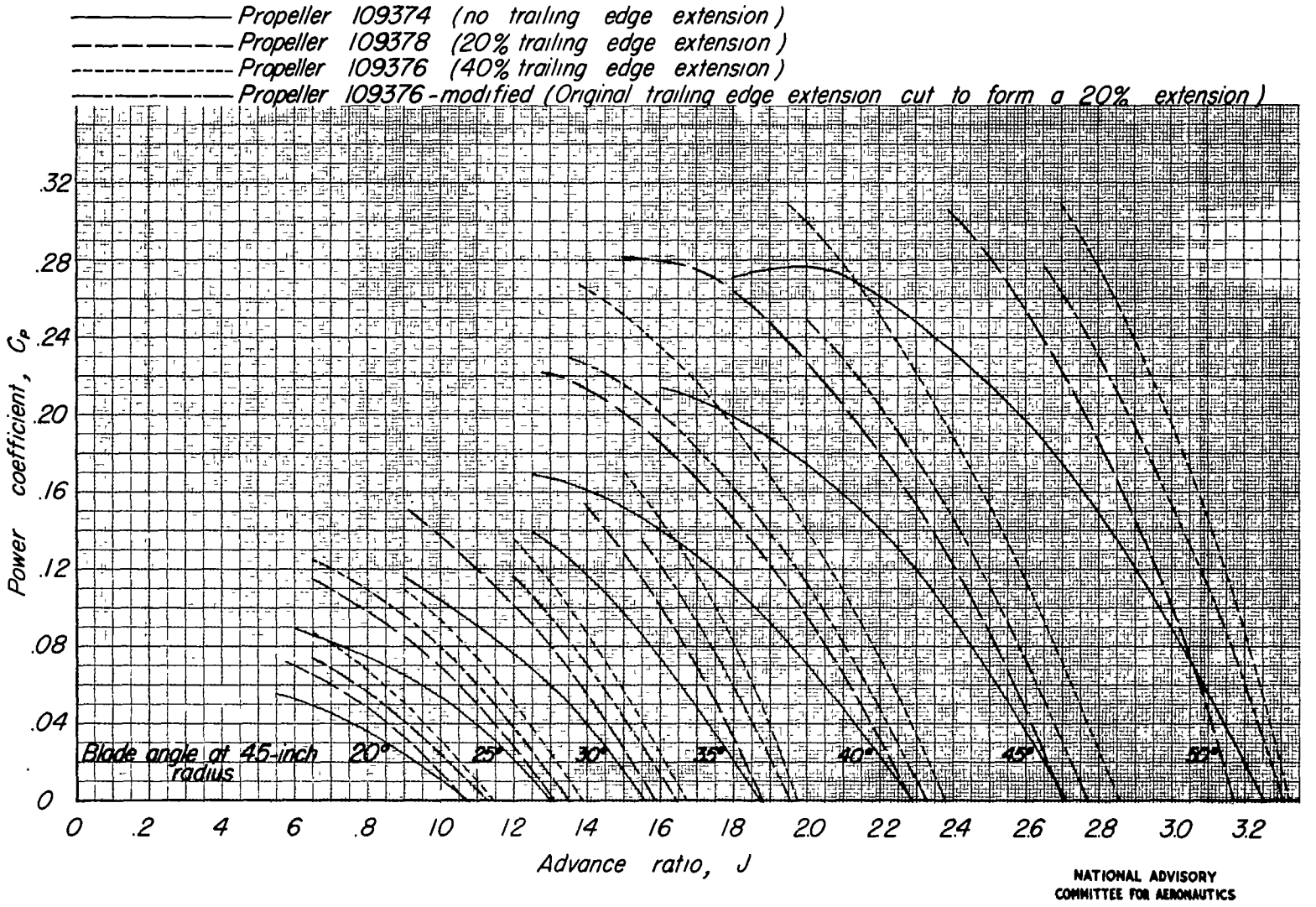

Figure 35 .—A comparison of the power coefficients for the four propellers tested

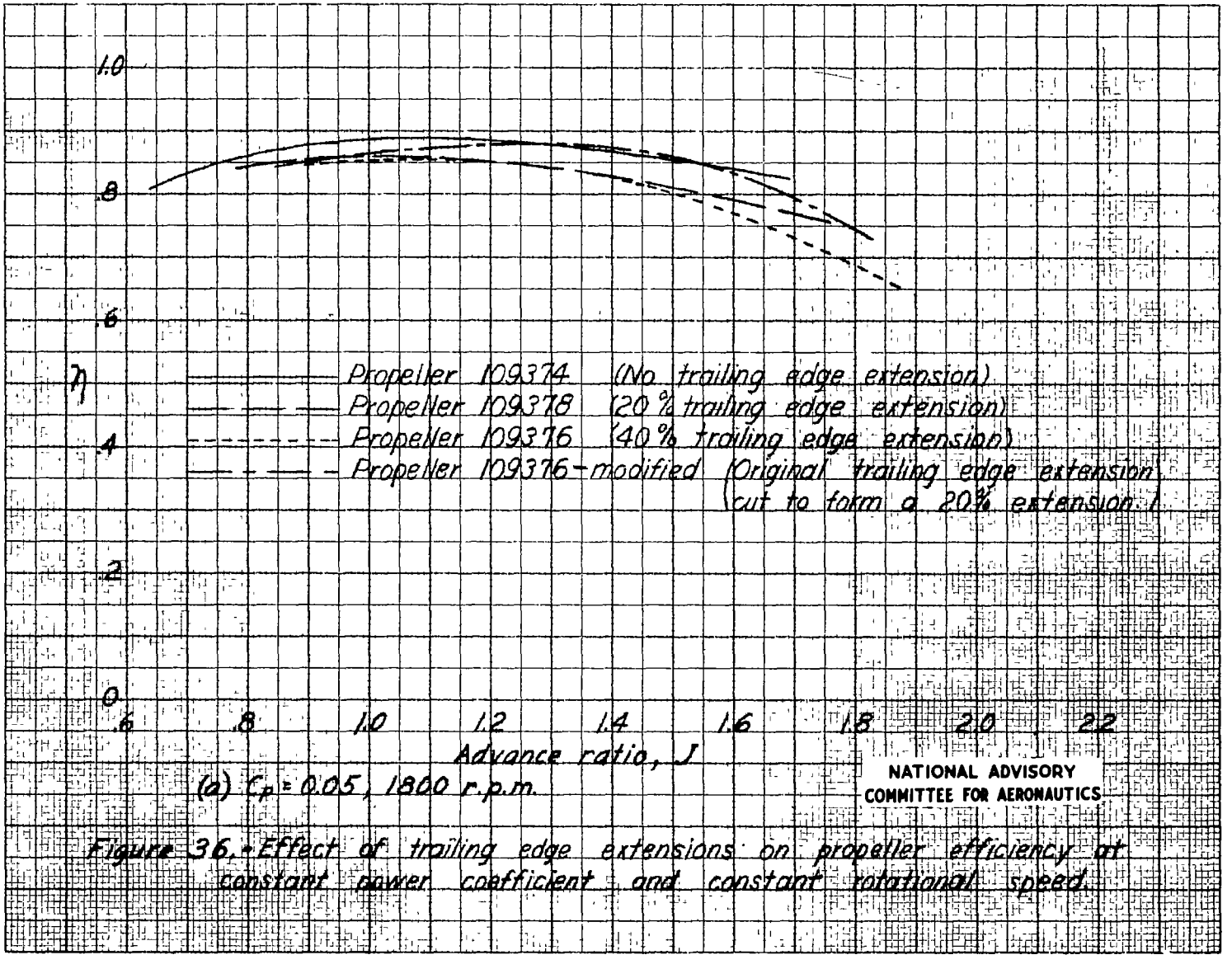

Figure 36.- Effect of trailing edge extensions on propeller efficiency at constant power coefficient and constant rotational speed.

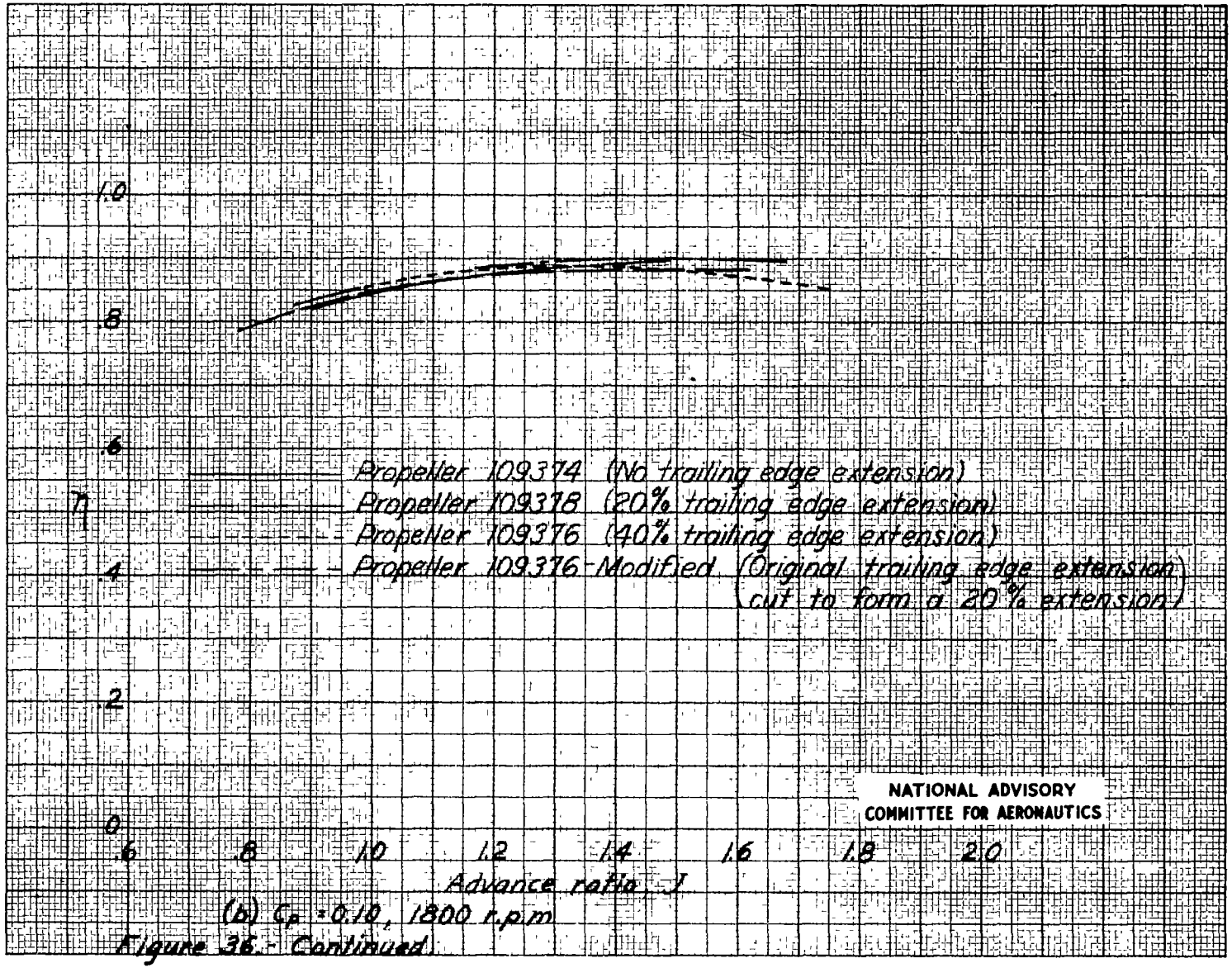

(b) $C_p = 0.10$, 1800 r.p.m

Figure 36.- Continued.

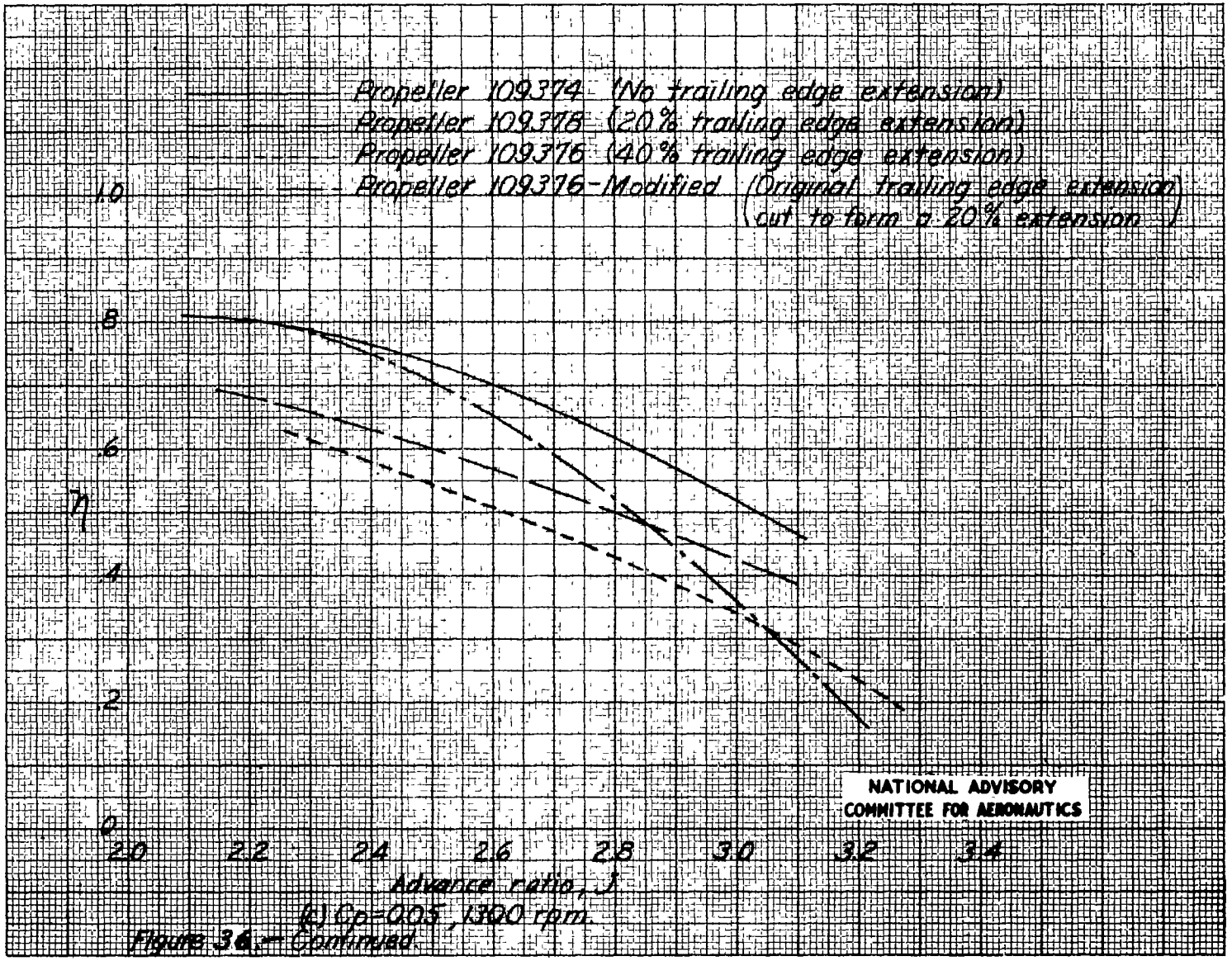

(f) C_p=.205, 1300 rpm.

Figure 36.- Continued.

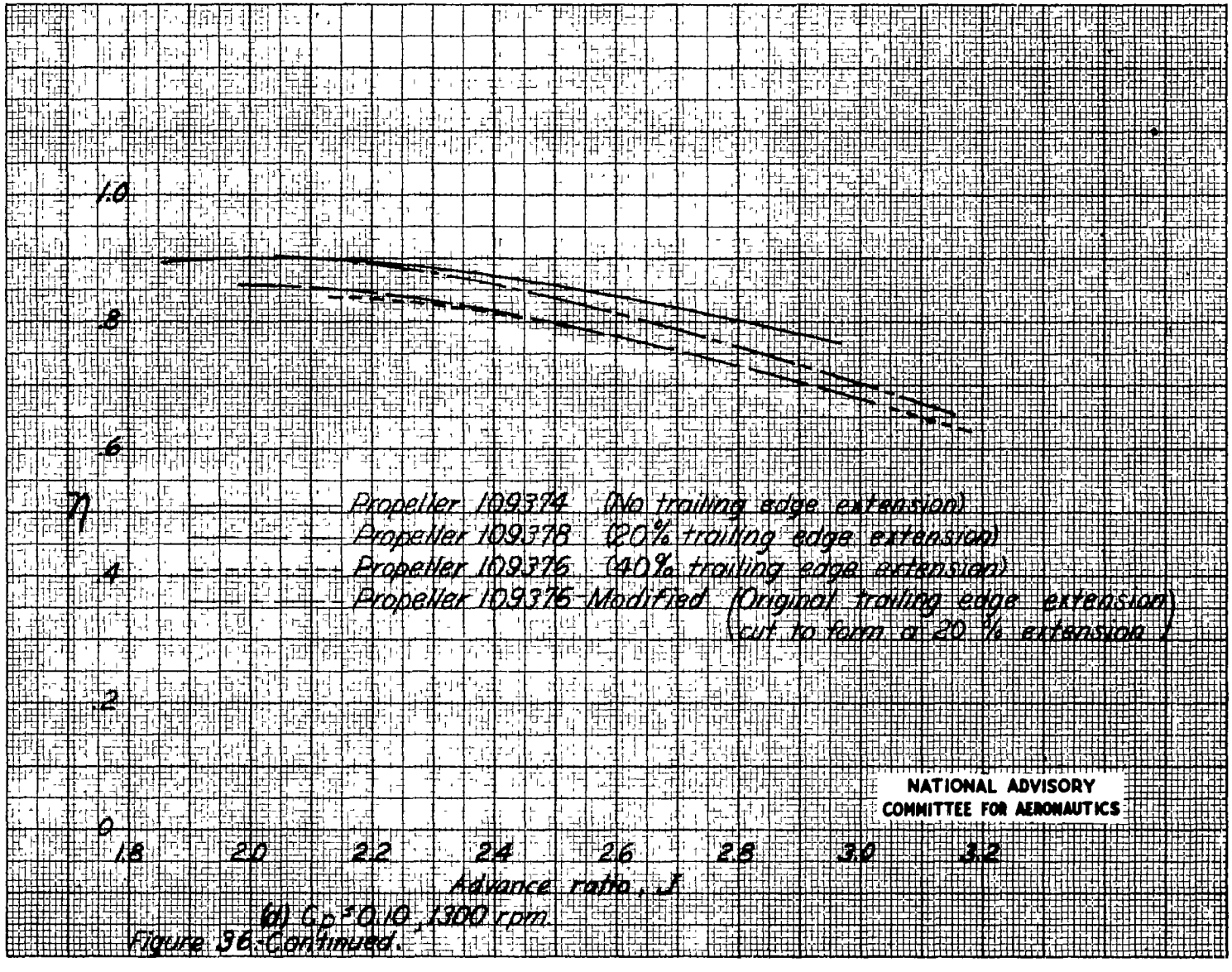

(d) C_p 0.10, 1300 rpm.

Figure 36.-Continued.

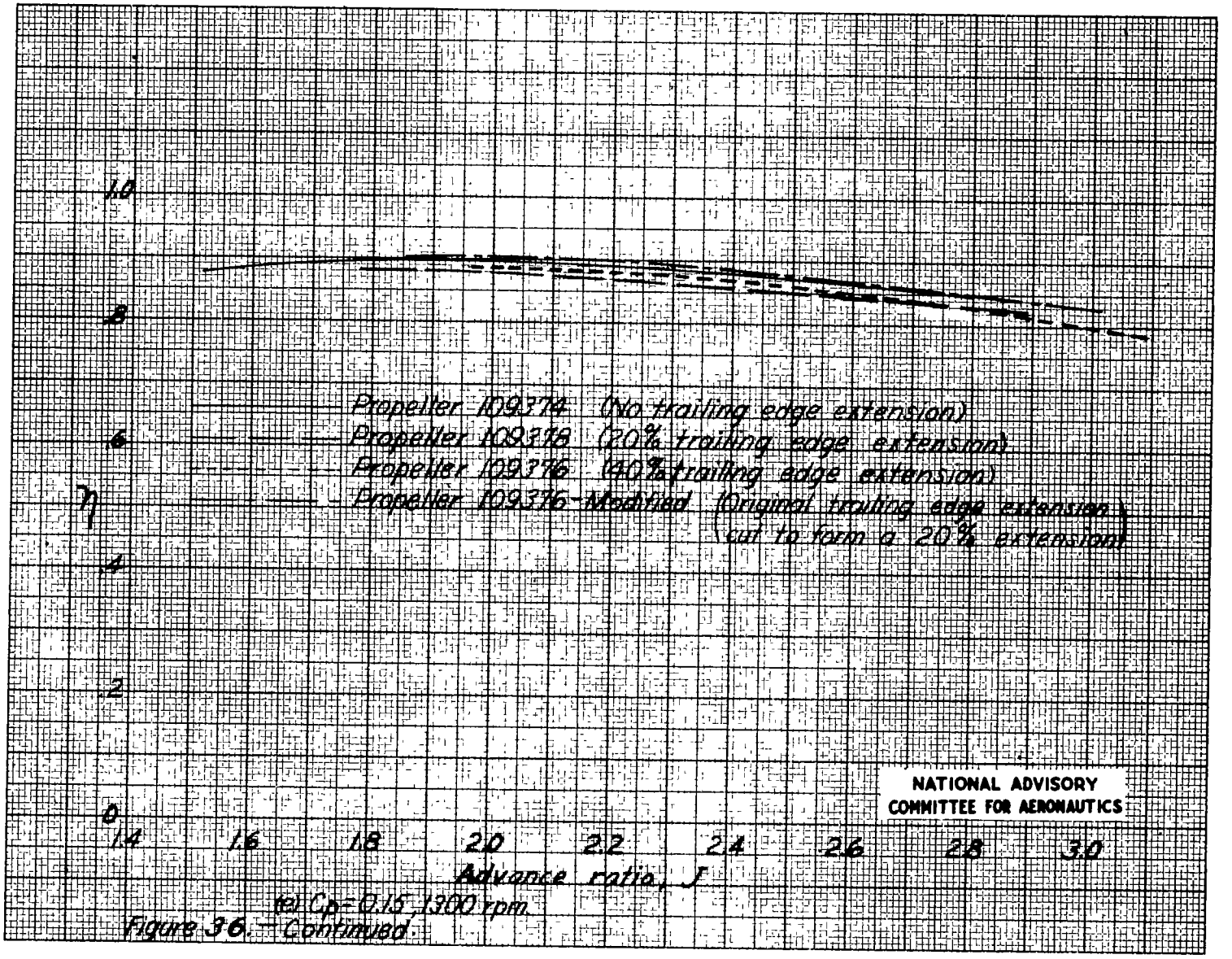

(e) C_p=0.15, 1300 rpm.

Figure 36.—Continued.

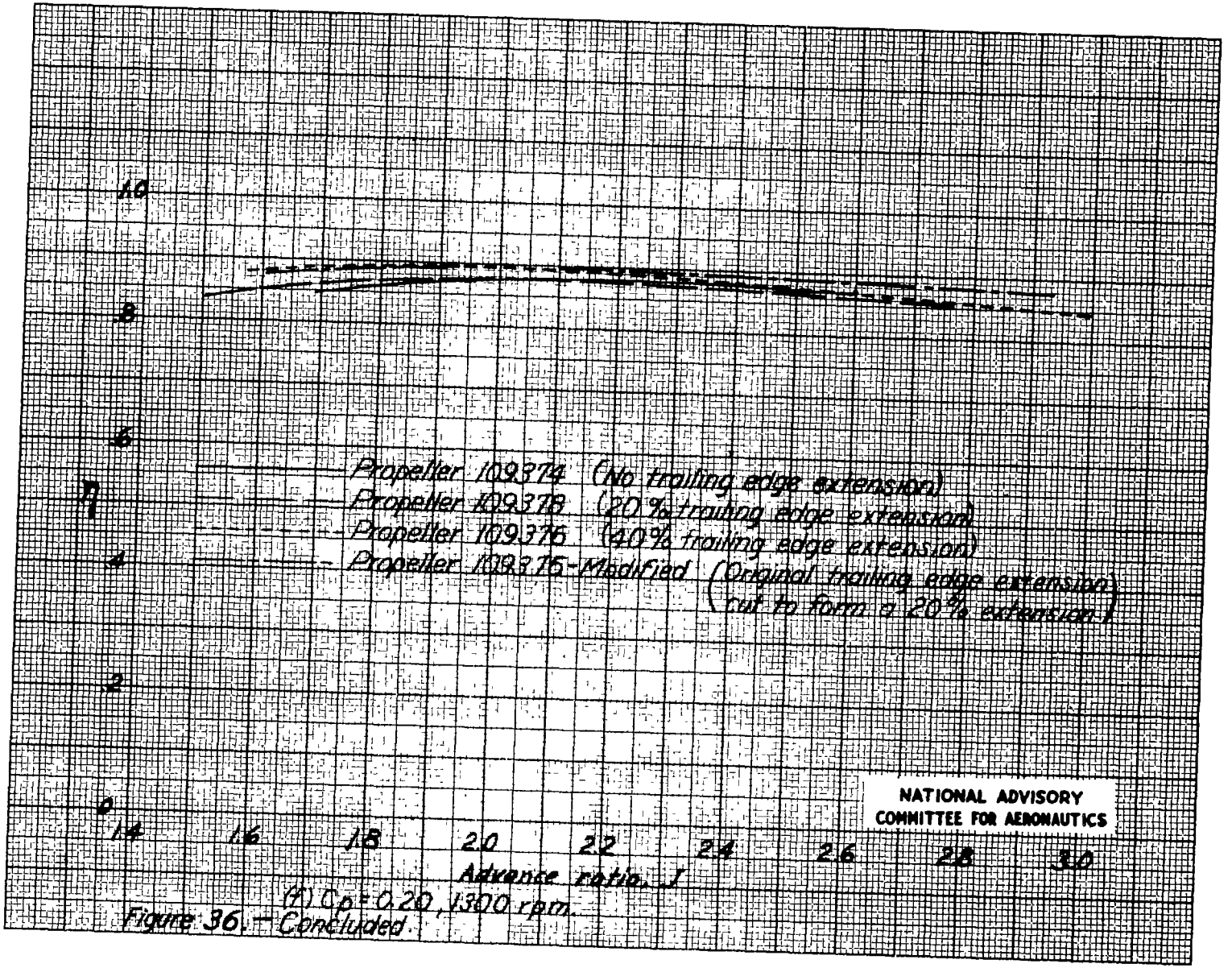

Figure 36.- Concluded.

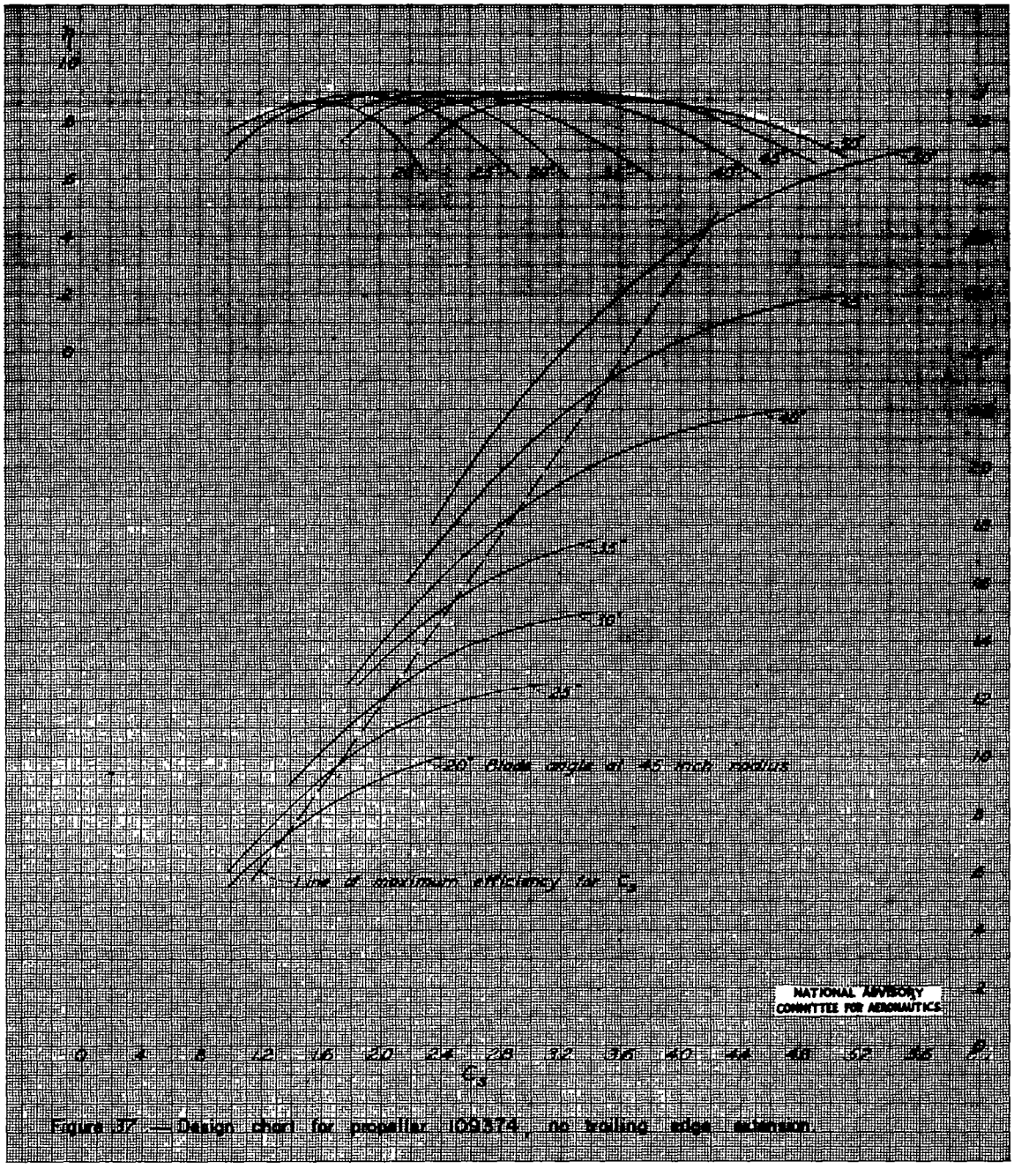

Figure 37.—Design chart for propeller 109374, no trailing edge extension.

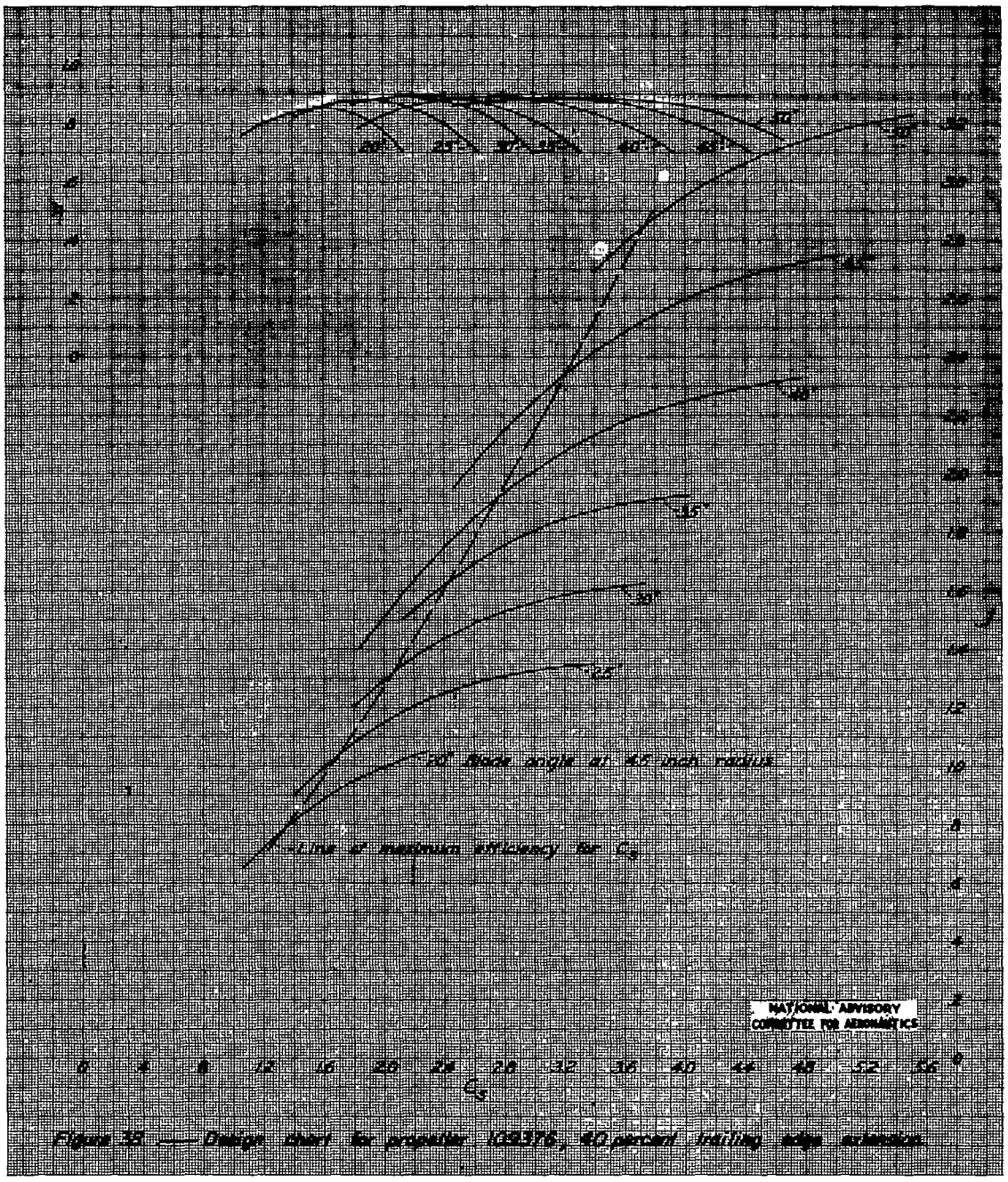

Figure 38.—Design chart for propeller 103376, 40 percent inviting edge extension.

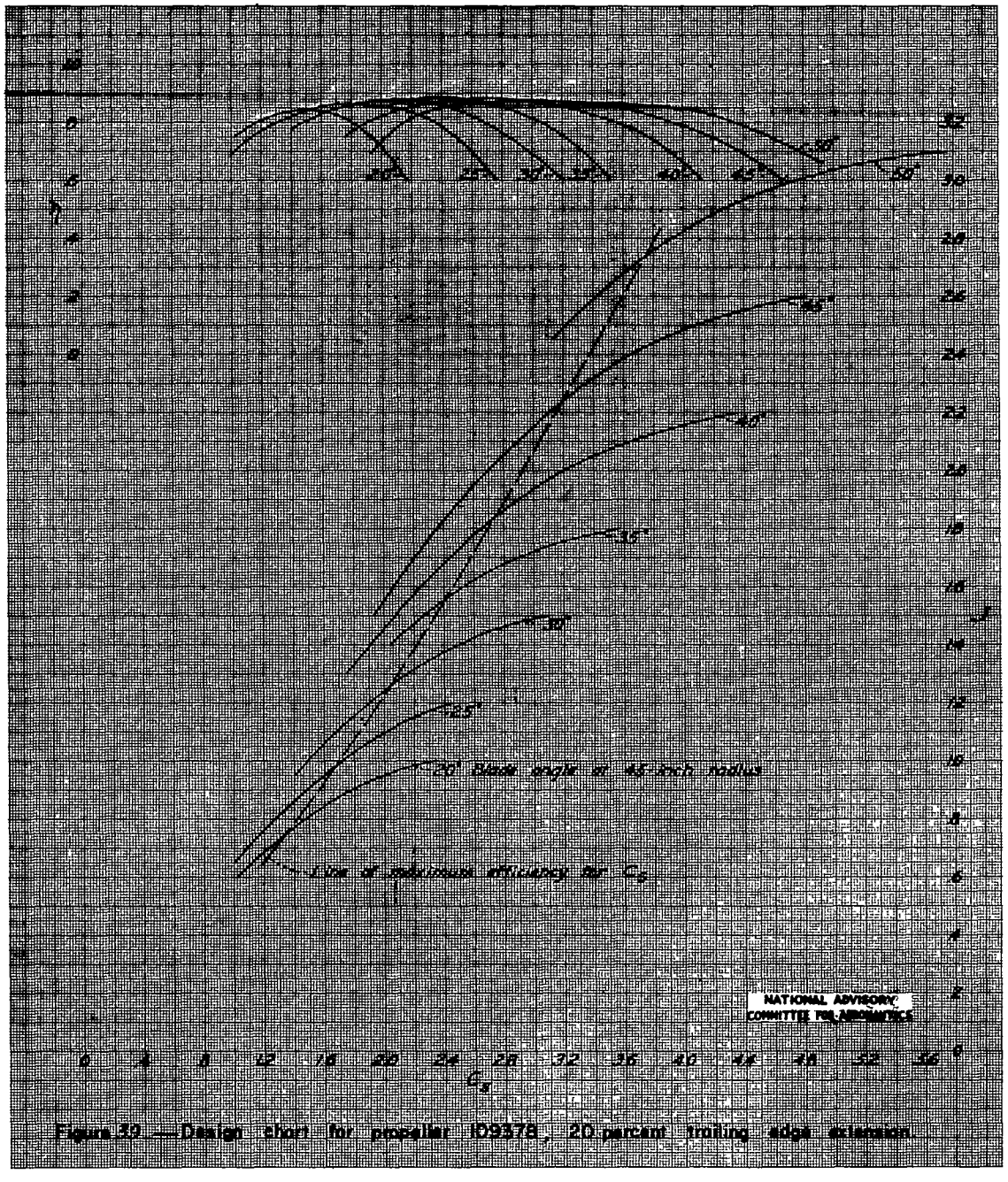

Figure 39.—Design chart for propeller 109378, 20 percent trailing edge extension.

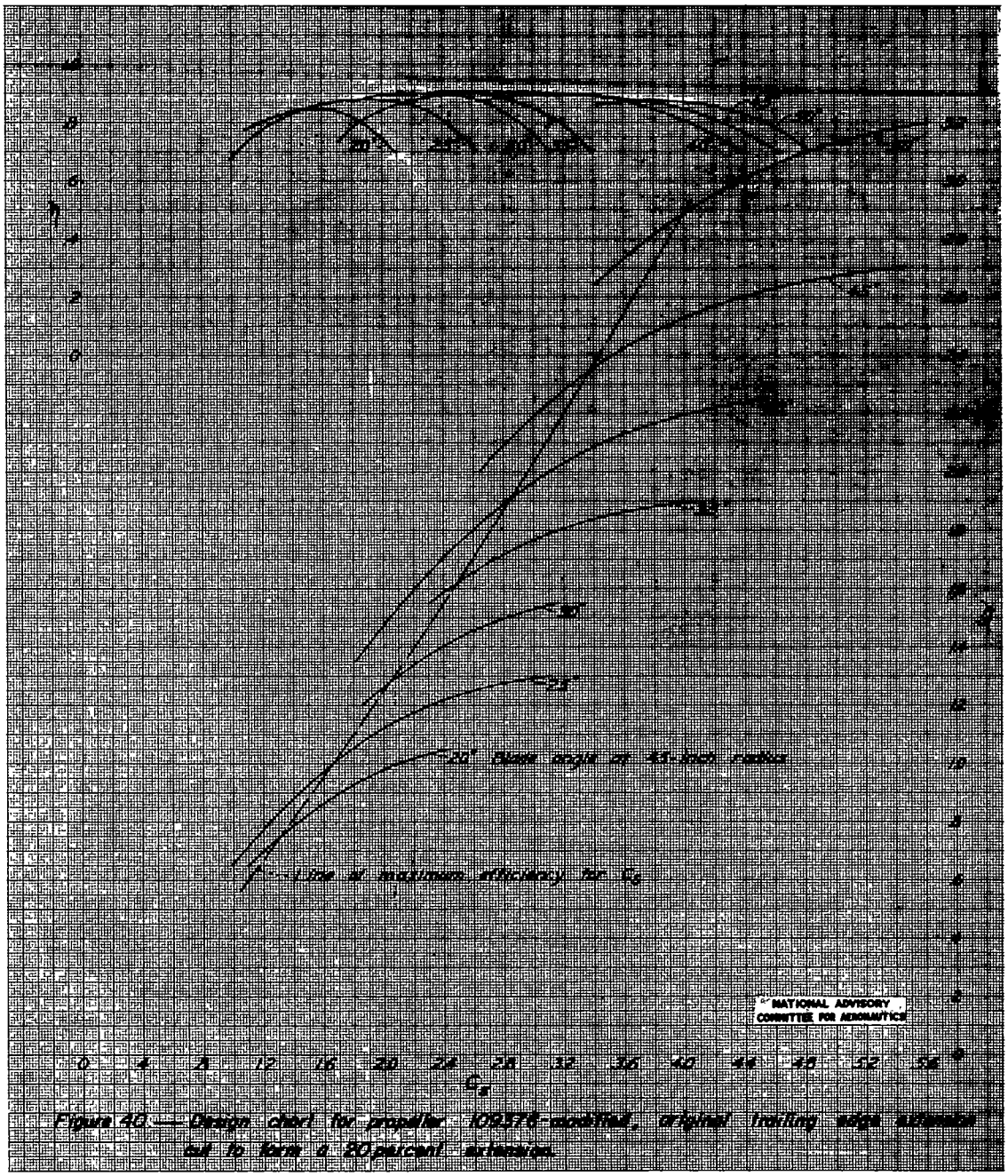

Figure 40.— Design chart for propeller 109176-modified, original trailing edge extension cut to form a 20-percent extension.

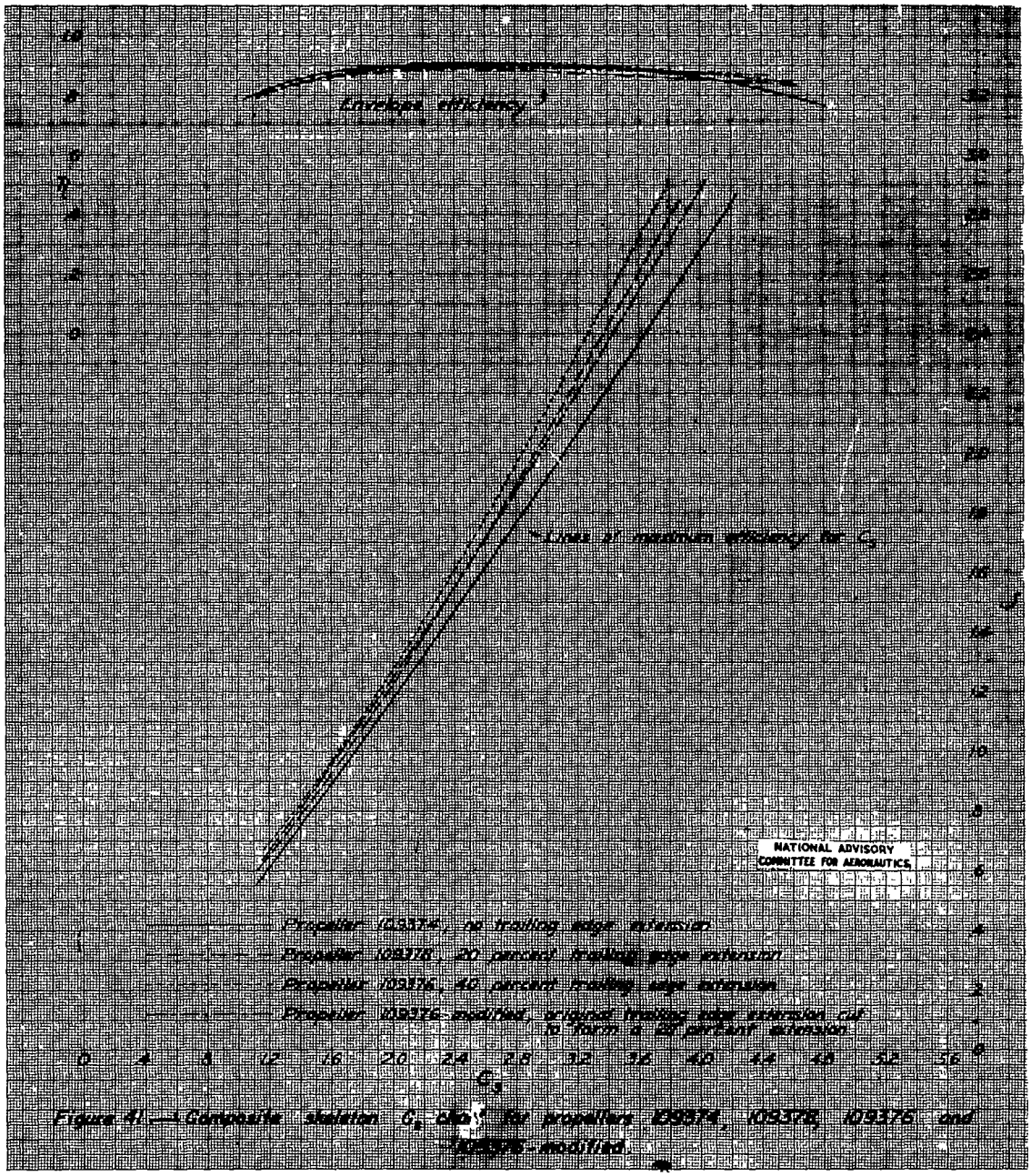

Figure 41.—Composite skeleton C_s chart for propellers 103374, 103376, 103376, and 103376-modified.